

1 **High number concentrations of transparent exopolymer particles (TEP) in**
2 **ambient aerosol particles and cloud water – A case study at the tropical**
3 **Atlantic Ocean**

4
5 **Manuela van Pinxteren¹, Tiera-Brandy Robinson², Sebastian Zeppenfeld¹, Xianda Gong³⁺,**
6 **Enno Bahlmann⁴, Khanneh Wadinga Fomba¹, Nadja Triesch¹, Frank Stratmann³, Oliver Wurl²,**
7 **Anja Engel⁵, Heike Wex³, Hartmut Herrmann^{1*}**

8
9 *Corresponding author: Hartmut Herrmann (herrmann@tropos.de)

10
11 ¹ Atmospheric Chemistry Department (ACD), Leibniz-Institute for Tropospheric Research
12 (TROPOS), 04318 Leipzig, Germany

13 ² Institute for Chemistry and Biology of the Marine Environment, Carl-von-Ossietzky
14 University Oldenburg, 26382 Wilhelmshaven, Germany

15 ³ Dept. of Experimental Cloud and Microphysics, Leibniz-Institute for Tropospheric Research
16 (TROPOS), 04318 Leipzig, Germany

17 + now at: Center for Aerosol Science and Engineering, Department of Energy, Environmental
18 and Chemical Engineering, Washington University in St. Louis, 63130, MO, USA

19 ⁴ Leibniz Centre for Tropical Marine Research (ZMT), 28359 Bremen, Germany

20 ⁵ GEOMAR Helmholtz Centre for Ocean Research, Kiel 24105, Germany

21

22

23

24

25

26

27

28

29

30

31

32

33

34 Abstract

35 Transparent exopolymer particles (TEP) exhibit the properties of gels and are ubiquitously
36 found in the world oceans. Possibly, TEP may enter the atmosphere as part of sea spray
37 aerosol. Here, we report number concentrations of TEP with a diameter $> 4.5 \mu\text{m}$, hence
38 covering a part of the supermicron particle range, in ambient aerosol and cloud water samples
39 from the tropical Atlantic Ocean as well as in generated aerosol particles using a plunging
40 waterfall tank that was filled with the ambient seawater. The ambient TEP concentrations
41 ranged between 7×10^2 and $3 \times 10^4 \text{ \#TEP m}^{-3}$ in the aerosol particles and correlations to sodium
42 (Na^+) and calcium (Ca^{2+}) ($R^2 = 0.5$) suggested some contribution via bubble bursting. Cloud
43 water TEP concentrations were between 4×10^6 and $9 \times 10^6 \text{ \#TEP L}^{-1}$ and, according to the
44 measured cloud liquid water content, corresponding to equivalent air concentrations of $2 -$
45 $4 \times 10^3 \text{ \#TEP m}^{-3}$.

46 Based on Na^+ concentrations in seawater and in the atmosphere, the enrichment factor for
47 TEP in the atmosphere was calculated. The tank-generated TEP were enriched by a factor of
48 50 compared to seawater and, therefore, in-line with published enrichment factors for
49 supermicron organic matter in general and TEP specifically. TEP enrichment in the ambient
50 atmosphere was on average 1×10^3 in cloud water and 9×10^3 in ambient aerosol particles and
51 therefore about two orders of magnitude higher than the corresponding enrichment from the
52 tank study. Such high enrichment of supermicron particulate organic constituents in the
53 atmosphere is uncommon and we propose that atmospheric TEP concentrations resulted
54 from a combination of enrichment during bubble bursting transfer from the ocean and a
55 secondary TEP in-situ formation in atmospheric phases. Abiotic in-situ formation might have
56 occurred from aqueous reactions of dissolved organic precursors that were present in particle
57 and cloud water samples, while biotic formation involves bacteria, which were abundant in
58 the cloud water samples.

59 The ambient TEP number concentrations were two orders of magnitude higher than recently
60 reported ice nucleating particle (INP) concentrations measured at the same location. As TEP
61 likely possess good properties to act as INP, in future experiments it is worth studying if a
62 certain part of TEP contributes a fraction of the biogenic INP population.

63

64 Keywords: Transparent exopolymer particles, marine aerosol particles, cloud water, plunging
65 waterfall tank, ice nucleating particles, Atlantic Ocean, Cape Verde Atmospheric Observatory
66 (CVAO)

67

68

69

70 1 Introduction

71 In marine ecosystems, polymer gels and gel-like material play an important role in the
72 biochemical cycling of organic matter (OM) (Passow, 2000, 2002b). One type of gel-like
73 particles, transparent exopolymer particles (TEP), have increasingly received attention. TEP
74 exist as individual particles rather than diffuse exopolymeric organic material and are
75 operationally defined as particles that are stained on 0.2 or 0.4 μm pore-sized polycarbonate
76 filters with the dye Alcian Blue (Passow, 2002b). TEP have shown surface-active properties
77 and are highly hydrated molecules (Passow et al. 2002a). Chemically, they consist of
78 polysaccharide chains including uronic acids or sulphated monosaccharides that are bridged
79 with divalent cations (mostly calcium) (Alldredge et al., 1993;Bittar et al., 2018).

80 In contrast to solid particles, TEP have properties of gels; with similar constituents
81 (carrageenans, alginic acid, and xanthan) to those that form gels, spontaneously forming from
82 dissolved fibrillar colloids, and they can be broken up by Calcium chelators such as EDTA.
83 However, because TEP have not yet been seen to undergo phase transition they can officially
84 only be classified as gel-like particles (Verdugo et al., 2004). Regardless though, TEP have been
85 shown to be highly important in sedimentation processes and carbon cycling in the sea (Mari
86 et al., 2017), as well as highly prevalent in the sea surface microlayer (SML) (Robinson et al.,
87 2019a) with a potentially significant effect on air-sea release of marine aerosols.

88 Generally, TEP can be formed via two pathways. First, the biotic pathway happens via
89 a breakdown and secretion of precursor material from an organism or via a direct release as
90 particles from aquatic organisms, e.g. as metabolic-excess waste products when nutrients are
91 limited (Decho and Gutierrez, 2017;Engel et al., 2004;Engel et al., 2002). High TEP
92 concentrations are usually associated with phytoplankton blooms, with the majority of
93 precursor material being released by diatoms and to a lesser extent other plankton species.
94 However, bacteria are also associated with TEP production, although their exact role is still
95 not resolved (Passow, 2002a). Secondly, TEP form through abiotic pathways. These could be
96 spontaneous formation from dissolved organic precursors (e.g. dissolved polysaccharides)
97 that are released by aquatic organisms. The abiotic formation is enhanced by turbulent or
98 laminar shear (Engel et al., 2002;Passow, 2000). Recent studies confirmed that higher wind
99 speeds, forming breaking waves, could be an effective transport and formation mechanism
100 for TEP to the ocean surface (Robinson et al., 2019b).

101 TEP are highly sticky and provide surfaces for other molecules and bacterial
102 colonization (Passow, 2002b), with between 0.5 and 25% (on average 3%) of marine bacteria
103 being attached to TEP (Busch et al., 2017). TEP naturally aggregate to other particles or highly
104 dense matter and can sink in the ocean to contribute to downward carbon fluxes (Logan et
105 al., 1995;Mari et al., 2017). However, TEP which are not attached to sufficiently dense material
106 will have a resulting low density and rise to the surface to form or stabilize the SML which links
107 the oceans with the atmosphere (Wurl and Holmes, 2008;Wurl et al., 2011).

108 From the ocean surface, TEP have the potential to be transferred to the air. Due to
109 wind and breaking waves, sea spray aerosol particles are formed (de Leeuw et al.,

110 2011;Lewandowska and Falkowska, 2013;Liss and Johnson, 2014) that could be a transfer
111 mechanism for TEP from the ocean to the atmosphere. Recently, high TEP mass
112 concentrations of $1.4 \mu\text{g m}^{-3}$ were reported in ambient marine aerosol particles measured in
113 a size range between 0.1 and $1 \mu\text{m}$, suggesting that gel-like particles can constitute more than
114 half of the particulate OM mass (Aller et al., 2017).

115 Ocean-derived OM, of which TEP is a part, has been reported to be enriched and
116 selectively transferred (compared to sea salt) to the atmosphere (Facchini et al., 2008;Keene
117 et al., 2007;van Pinxteren et al., 2017). Compared to seawater concentrations, organic mass
118 in submicron aerosol particles is strongly enriched by factors of 10^3 and 10^4 (partly up to 10^5)
119 (Quinn et al., 2015 and references therein) due to (not yet in detail resolved) processes during
120 the rise and burst of bubbles at the ocean surface (Blanchard, 1975). The enrichment of OM
121 in supermicron aerosol particles is significantly lower, with average aerosol enrichment factors
122 of 10^2 (Hoffman and Duce, 1976;Keene et al., 2007;Quinn et al., 2015). Aerosol enrichments
123 have been studied for several organic compound groups such as lipids, carbohydrates, and
124 proteins (e.g. Gao et al., 2012;Rastelli et al., 2017;Schmitt-Kopplin et al., 2012;Triesch et al.,
125 2021a;Triesch et al., 2021b;Zeppenfeld et al., 2021). However, at current, data for TEP
126 enrichment in the atmosphere are scarce. Aller et al. (2017) presented TEP mass
127 concentrations in size-resolved aerosol particles and found them to contain more TEP for
128 submicron sizes than for larger sizes. Kuznetsova et al. (2005) reported TEP enrichment of a
129 factor of 40 in freshly produced sea spray. Besides TEP, other types of gel-like airborne
130 particles in the size range of 100 – 300 nm (and even smaller) have been observed, e.g. in the
131 Arctic atmosphere likely originating from the ocean surface (Bigg and Leck, 2008;Leck and
132 Bigg, 2005a, b).

133 In addition to an oceanic transfer, atmospheric in-situ formation might contribute to
134 OM abundance in the atmosphere. Ervens and Amato (2020) provided a framework to
135 estimate the production of secondary biological aerosol mass in clouds by microbial cell
136 growth and multiplication. It was recently shown that this pathway might represent a
137 significant source of biological aerosol material (Ervens and Amato, 2020;Khaled et al.,
138 2021;Zhang et al., 2021). In another recent study, cloud water in-situ formation of amino acids
139 resulting from biotic and abiotic processes has been measured and modelled (Jaber et al.,
140 2021). Moreover, a higher microbial enzymatic activity on the aerosol particles compared to
141 seawater was observed and it was hypothesised that after ejection from the ocean, active
142 enzymes can dynamically influence the OM concentration and composition of marine aerosol
143 particles (Malfatti et al., 2019). Still, the atmospheric in-situ formation of important OM
144 compounds and its importance is not well investigated to date and no studies exist about
145 atmospheric in-situ TEP formation.

146 Regarding the properties of ocean-derived OM in the atmosphere, its ability to act as
147 cloud condensation nuclei (CCN) (Orellana et al., 2011;Sellegrri et al., 2021) or ice nucleating
148 particle (INP) (Burrows et al., 2013;Gong et al., 2020a;McCluskey et al., 2018a;McCluskey et
149 al., 2018b) is not well understood at present. Bigg and Leck, (2008) and Leck and Bigg (2005b)

150 demonstrated, based on morphology and chemical properties, that the biogenic particles
151 collected in air and in the surface microlayer could be consistent with polymer gels. For regions
152 that generally show a low total particle number concentration and low CCN (such as the high
153 Arctic), it was suggested that microgels are CCN (Leck and Bigg, 2005a, b; Orellana et al., 2011),
154 due to their hydrated and hygroscopic nature and due to the absence of other significant
155 aerosol particle sources.

156 In addition, oceanic biogenic INP sources have been discussed (Creamean et al.,
157 2019; Hartmann et al., 2020; Wilson et al., 2015; Zeppenfeld et al., 2019). In regions, however,
158 where other sources dominate, oceanic sources might not suffice to explain the INP
159 population, and non-marine sources most likely significantly contribute to the local INP
160 concentration (Gong et al., 2020a). According to their structure, biopolymers consisting of
161 proteins, lipids, and higher saccharides have been shown to play a role in the ice-nucleating
162 activity (Pummer et al., 2015). In this context, TEP might provide excellent functionalities to
163 act as INP, as they form a 3D network where water molecules can attach, providing a
164 structured surface for ice formation. A direct link between TEP and INP, however, has not yet
165 been experimentally shown in field studies.

166 Within the present study, the number concentrations and size distributions of TEP in
167 the ambient atmosphere in the tropical Atlantic Ocean were elucidated. We aimed at
168 investigating the TEP number concentrations in the ambient aerosol particles and cloud water
169 and to derive connections to oceanic transfer and potential in-situ formation mechanisms.
170 Finally, we compared the TEP number concentrations with recently published atmospheric
171 INP number concentrations at the same location (Gong et al., 2020a) and analyse possible
172 interconnections. To our knowledge, this is the first study with detailed measurements of TEP
173 number size distribution in different atmospheric marine compartments in the tropical
174 Atlantic environment.

175

176 2 Material and methods

177 2.1 Measurement site and ambient sampling

178 Samples were taken during the MarParCloud: “Marine biological production, organic
179 aerosol particles and marine clouds: a Process chain” campaign that took place from
180 September 13th to October 13th 2017 at the Cape Verde archipelago Island Sao Vicente located
181 in the Eastern Tropical North Atlantic (ETNA). A detailed overview of the campaign,
182 background, goals, and first results are available in van Pinxteren et al. (2020). Measurements
183 were performed at the Cape Verde Atmospheric Observatory (CVAO) as described in more
184 detail elsewhere (Triesch et al., 2021a; Triesch et al., 2021b; van Pinxteren et al., 2020). The
185 CVAO is located directly at the shoreline at the northeastern tip of the São Vicente island at
186 10 m a.s.l (Carpenter et al., 2010; Fomba et al., 2014). Due to the trade winds, this site is free
187 from local island pollution and provides reference conditions for studies of ocean-atmosphere

188 interactions as there is a constant north-westerly wind from the open ocean towards the
189 observatory. However, it also lies within the Saharan dust outflow corridor, and mainly in the
190 winter months (January and February), dust outbreaks frequently occur.

191 Total suspended aerosol particle (TSP) for TEP analysis and PM₁₀ sampling for analysis
192 of further aerosol constituents (inorganic ions, INP, dust) was performed on top of a 30 m
193 sampling tower of the CVAO. Tower measurements there mainly represent the conditions
194 above the ocean because the internal boundary layer (IBL), which can form when air passes a
195 surface with changing roughness (i.e. the transfer from open water to island), is mainly
196 beneath 30 m (Niedermeier et al., 2014). During the MarParCloud campaign, the marine
197 boundary layer (MBL) was well mixed as indicated by an almost uniform particle number size
198 distribution within the MBL (Gong et al., 2020b; van Pinxteren et al., 2020). Information on the
199 meteorological conditions during the sampling period is given in **Tab. S1**.

200 TSP were sampled with a filter sampler consisting of a filter holder equipped with a
201 0.2 µm pore-sized polycarbonate (PC) filter mounted to a pump. The PC filters had been
202 cleaned with 10% HCl and rinsed with ultrapure water (resistivity=18.2MΩ cm) before
203 application. Sampling usually took place for 24 h and the flow of the pump was between 5 and
204 10 L min⁻¹ and frequently measured with a flowmeter. Total volumes between 10 and 15 m³
205 were sampled. In seawater TEP analysis, filtration is usually performed at a gentle pressure of
206 0.2 bar (Engel, 2009) which corresponds to a max flow rate of 21 or 38 L min⁻¹. The flow rate
207 of aerosol sampling was max. 10 L min⁻¹ and therefore TEP losses during aerosol particle
208 sampling were not expected.

209 PM₁₀ particles were sampled with a high volume sampler (Digitel, Riemer, Germany)
210 equipped with preheated (105 °C for 24 h) 150 mm quartz fiber filters (Munktell, MK 360) at
211 a flow rate of 700 L min⁻¹, described in detail elsewhere (van Pinxteren et al., 2020). The
212 sampling times for TSP as well as PM₁₀ were usually set to 24 h.

213 Cloud water was sampled on Mt. Verde, which is the highest point of the São Vicente
214 Island (744 m), situated in the northeast of the Island (16°52.11'N, 24°56.02'W) and northwest
215 to the CVAO (van Pinxteren et al., 2020). Again, Mt. Verde experiences direct trade winds from
216 the ocean with no significant influence of anthropogenic activities from the island (Carpenter
217 et al., 2010). Bulk cloud water was collected using a compact Caltech Active Strand Cloudwater
218 Collectors (CASCC2) equipped with acid cleaned Teflon®strands (508 µm diameter). Cloud
219 droplets were caught on the strands and gravitationally channelled into an Nalgene bottle.
220 The 50% lower size cut for the CASCC2 is approximately 3.5 µm diameter. Much of the liquid
221 water content (LWC) in clouds is contained of drops between 10 and 30 µm diameter and the
222 CASCC2 is predicted to collect drops in this size range with an efficiency greater than 80%
223 (Demoz et al., 1996).

224 Three cloud water samples collected on the 20.09.2017, the 28.09.2017, and the
225 04.10.2017 were analysed for the TEP number concentrations. They were filtered (150-200
226 mL) through 0.2 µm pore-sized filters for TEP analysis using the same filter type and conditions
227 as applied for the aerosol particle staining. All equipment that was in contact with the cloud

228 water samples (Teflon® strands, sampling bottles, filters) had been cleaned with 10% HCl and
229 rinsed with ultrapure water (resistivity=18.2MΩ cm) before each application as recommended
230 in Engel (2009).

231

232 2.2. Particle sampling from the plunging waterfall tank

233 To investigate a direct oceanic transfer of TEP via bubble bursting, TSP particles were
234 sampled from a plunging waterfall tank experiment that is described in detail in the
235 MarParCloud overview paper (van Pinxteren et al., 2020, SI section). The tank was designed
236 to study the bubble-driven transfer of organic matter from the bulk water into the aerosol
237 phase. It consists of a 1400 L basin with a 500 L aerosol chamber on top. The bubble driven
238 transport of organic matter was induced using a skimmer on a plunging waterfall. A stainless
239 steel inlet was inserted in the headspace of the tank and connected with three filter holders
240 for offline aerosol particle sampling without size segregation (TSP). The filter system for TEP
241 analysis was equipped with a 0.2 μm pore-sized, acid-cleaned polycarbonate (PC) filter
242 mounted to a pump. Sampling usually took place for ~ 24 h, the flow of the pump was between
243 5 and 10 L min⁻¹ and frequently measured with a flowmeter. Total volumes between 9 and
244 10 m³ were sampled. The sampling procedure was therefore identical to the ambient TEP filter
245 sampling. Another filter holder was equipped with a preheated 47 mm quartz fiber filter
246 (Munktell, MK 360) for sodium analysis. The stainless steel inlet was additionally connected
247 to a TROPOS-type Scanning Mobility Particle Sizer (Wiedensohler et al., 2012) for online
248 aerosol measurements. This method of aerosol generation resulted in an efficient generation
249 of nascent sea-spray aerosol particles with an aerosol particle size distribution centred around
250 100 nm (van Pinxteren et al. 2020).

251

252 2.3 Analysis

253 The filters obtained from ambient and tank-generated TSP aerosol particle sampling
254 and cloud water filtrations were stained with 3 mL of an Alcian blue stock solution (0.02 g
255 Alcian blue in 100 mL of acetic acid solution, pH 2.5) for 5 s yielding an insoluble non-ionic
256 pigment and afterward rinsed with milliQ water. The dye Alcian blue consists of a
257 macromolecule with a central copper phthalocyanine ring linked to four isothiuronium
258 groups via thioether bonds (Passow and Alldredge, 1995). The isothiuronium groups are
259 strong bases and account for the cationic nature. The exact staining mechanism is not resolved
260 but it is believed that the cationic isothiuronium groups bond via electrostatic linkages (ionic
261 bonds) with the polyanionic molecules of the TEP molecule, hence the carboxylic and sulfonic
262 side groups are stained. Alcian Blue can also react with carbohydrate-conjoined proteins at
263 proteoglycans, but not with nucleic acids and neutral biopolymers (Villacorte et al., 2015).
264 After staining the filters were kept at -20°C and transported to the laboratories of TROPOS.

265 For microscopic analysis, the protocol following Engel (2009) was applied. In short,
266 abundance, area, and size-frequency distribution of TEP were determined using a light
267 microscope (Zeiss Axio Scope A.1) connected to a camera (ColorView III). Filters were screened
268 at 200× magnification. About 10 pictures were taken randomly from each filter in two
269 perpendicular cross-sections (5 pictures each cross-section; dimension 2576 x 1932 pixel, 8-
270 bit color depth) and microscopic pictures of TEP in cloud water are shown in **Fig. 1**. Images
271 were then semi-automatically analyzed using ImageJ (Version 1.44). A minimum threshold
272 value of 16 μm^2 was set for particle size during particle analysis to remove the detection of
273 non-aggregate material by the program. This resulted in a minimum particle size of 4.5 μm
274 (assuming spherical particle).

275

276 ***Insert Figure 1***

277

278 Blank filters were taken for aerosol sampling (inserting filters in the aerosol sampler
279 without probing them) and cloud water (filtering reagent water over a pre-cleaned filter),
280 stained and treated the same way as the microscopic analysis. Blank number concentrations
281 were on average 6% of the cloud water results and between 5% and 20% for aerosol results
282 and the blank values were subtracted from the samples.

283 The analysis of inorganic ions from PM_{10} samples was performed with ion
284 chromatography and conductivity detection. Aqueous extracts of the aerosol samples were
285 made by ca. 25% of the PM_{10} filter in 1.5 mL ultra-pure water (resistivity = 18.2 $\text{M}\Omega\text{ cm}$) for
286 one hour. After the filtration (0.45 μm syringe filter) of the extracts sodium (Na^+), calcium
287 (Ca^{2+}), magnesium (Mg^{2+}), were analyzed by using ion chromatography (Dionex ICS-6000,
288 Thermo Scientific). The cations were separated in an isocratic mode (eluent: 36 mM
289 methanesulfonic acid) on a Dionex IonPac CS16-4 μm column (2×250 mm) that was combined
290 with a Dionex IonPac CG16-4 μm guard column (2×50 mm). The detection limits for the
291 determined ions were between 5 and 20 $\mu\text{g L}^{-1}$ (Zeppenfeld et al., 2021).

292 Non-sea-salt calcium was calculated from the ion ratio of $\text{Ca}^{2+}/\text{Na}^+$ in seawater of
293 0.038 (Turekian, 1968). Dust concentrations were estimated from the aerosol particle mass
294 concentrations as the residual mass after the subtraction of all analytical concentrations from
295 the PM_{10} mass as described elsewhere (Fomba et al., 2014). Trace metal content was
296 determined using a Total Reflection X-Ray Fluorescence (TXRF) S2 PICOFOX (Bruker AXS,
297 Berlin, Germany) spectrometer equipped with a Molybdenum X-ray source (Fomba et al.,
298 2013). The cloud LWC was measured with a particle volume monitor (PVM-100, Gerber
299 Scientific, USA), which was mounted at the same height as the cloud water samplers.

300 INP number concentration (N_{INP}) were measured with two droplet freezing techniques
301 (LINA: Leipzig Ice Nucleation Array and INDA: Ice Nucleation Droplet Array) in different marine
302 compartments. The uncertainties of N_{INP} are given by the 5% to 95% confidence interval and
303 the results are presented in (Gong et al., 2020a).

304 All the samples of this study are summarized in Table 1. In addition to samples from
305 the MarParCloud campaign, surface seawater samples obtained from the ETNA (Engel et al.
306 2020) were considered.

307 **Insert Table 1**

308 2.4 Enrichment factor

309 To determine enrichment or depletion of TEP in the atmosphere (i.e. on the aerosol
310 particles and in the cloud water) in relation to the TEP concentration in the ocean water, the
311 concept of the aerosol enrichment factor can be applied. To this end, the concentration of the
312 compound of interest in each compartment is related to the respective sodium mass
313 concentration, as sodium is regarded as a conservative sea salt tracer transferred to the
314 atmosphere in the process of bubble bursting (Sander et al., 2003). This concept is usually
315 applied for calculating the enrichment of a compound in the aerosol particles ($EF_{aer.}$) in relation
316 to seawater (Quinn et al., 2015), but was recently extended to calculate the enrichment of
317 organic compounds in cloud water (EF_{cloud}) in relation to seawater (Triesch et al., 2021a).
318 Therefore, in the following the enrichment factor is defined as $EF_{atm.}$ (atmosphere
319 enrichments factor) in equation 1.

320

$$321 \quad EF_{atm.} = \frac{c(TEP)_{atm}/c(Na^{+mass})_{atm}}{c(TEP)_{seawater}/c(Na^{+mass})_{seawater}} \quad (1)$$

322

323 For equation (1), TEP number concentrations were converted to TEP volume
324 concentrations. To this end, for atmospheric and for oceanic samples, particle number
325 concentrations of TEP were extracted from the size distribution spectra and volume
326 concentrations were calculated (assuming spherical particles). More detail on the conversion
327 can be found in the SI (Tab. S2-S5).

328

329 3 Results and Discussion

330 3.1 Concentration and size distribution of TEP

331 Within the three-weeks sampling period, TEP varied within one order of magnitude
332 between 7×10^2 and 3×10^4 #TEP m^{-3} in the aerosol particles and between 4×10^6 and 9×10^6
333 #TEP L^{-1} in the cloud water (analysed diameter size range: ~ 4.5 to ~ 30 μm) as shown in **Fig. 2**.
334 The cloud water concentrations were converted to atmospheric concentrations using the
335 measured LWC of the cloud water (0.39 $g\ m^{-3}$) and resulted in concentrations of $2 - 4 \times 10^3$
336 #TEP m^{-3} (**Tab. S4**). Comparing the #TEP concentrations in cloud water to the ones in the
337 ambient aerosol particles suggested that about 20% of the ambient TEP particles are activated
338 to cloud droplets when a cloud forms.

339 **Insert Figure 2**

340

341 In addition, TEP were measured in four aerosol particle samples from the plunging
342 waterfall tank and the concentrations varied between 4×10^2 and 3×10^3 #TEP m^{-3} (**Tab. S3**).
343 While the TEP concentrations in ambient aerosol particle and cloud water were not
344 significantly different (ANOVA, oneway, $p = 0.054$ at a 0.05 level), the tank-generated TEP
345 concentrations were significantly lower than the ambient aerosol TEP concentrations (ANOVA,
346 oneway, $p = 0.004$ at a 0.05 level). The TEP number concentrations measured in the different
347 atmospheric compartments, the ambient aerosol particles, the tank-generated aerosol
348 particles and the cloud water are summarized in **Fig. 3a** and the individual values are
349 presented in the **Tab. S2-S4**.

350 *Insert Figure 3*

351

352 In addition to the total number concentrations, TEP number size distribution were
353 derived from all ambient aerosol particle samples and are shown in **Fig. 4 (a-d)** in both, linear
354 and logarithmic form. In addition, the TEP number size distribution of one cloud water sample
355 is presented in **Fig. 4 (e, f)**. All samples exhibited very similar trends in their size distribution,
356 with higher number concentrations for smaller sizes.

357 *Insert Figure 4*

358

359 From the observed size distributions, it can be assumed that the number
360 concentrations will continue to increase toward smaller sizes. A comparison of TEP number
361 concentrations in the ambient aerosol particles or cloud water to literature values is
362 challenging due to the availability of very few studies and different sample types and size
363 ranges regarded in different studies. However, the here observed trend in the TEP number
364 size distributions is consistent with studies from Kuznetsova et al. (2005) showing increased
365 TEP concentrations in simulated sea spray regarding particle sizes from $50 \mu\text{m}$ to $10 \mu\text{m}$ in
366 diameter. In addition, TEP mass concentrations showed a similar trend with higher
367 concentrations towards smaller particle sizes (size range $0.1\text{-}1 \mu\text{m}$, Aller et al. (2017)), that
368 was, however not as pronounced as for TEP number concentrations observed here.

369 Regarding polymer gels in general, a strong increase with decreasing sizes was
370 observed in cloud water in the high Arctic (north of 80°N) in late summer using a very sensitive
371 microscopic technique with epifluorescence (Orellana et al., 2011). 2×10^9 micrometer-sized
372 polymer gels per mL^{-1} and $2 - 6 \times 10^{11}$ nanometer-sized polymer gels per mL^{-1} were observed
373 and the majority of the particles were smaller than 100 nm (Orellana et al., 2011). The
374 measurements from Orellana et al. (2011) regarded a much smaller particle diameter range
375 (down to nm scale) compared to the present work and are therefore not directly comparable.
376 However, from the logarithmic TEP number concentration vs. diameter relationship (**Fig.4**) we
377 calculated TEP number concentrations for smaller particle ranges (sub-micrometer size

378 range). TEP number concentrations between 4.2×10^4 #TEP m^{-3} (low “TEP5” case, equation
379 from **Fig. 4b**) and 1.6×10^6 #TEP m^{-3} (high “TEP10” case, equation from **Fig. 4d**) are calculated
380 for 1 μm large particles. The high but varying concentrations for the two cases underlines the
381 need for more measurements in the submicron range to derive robust numbers. Similarly, a
382 concentration of 3.0×10^8 #TEP L^{-1} for 1 μm large particles in cloud water were calculated and
383 2.1×10^{10} #TEP L^{-1} for 200 nm large particles might exist in the submicron-size range (following
384 the equation from **Fig. 4f**).

385 These calculations show that the number of gel-like particles in the high Arctic was still
386 several orders of magnitudes higher compared to TEP particles in the tropical Atlantic, e.g.
387 10^{10} #TEP L^{-1} (200 nm particles) in tropical cloud water observed here vs. 10^{11} #polymer gels
388 per mL^{-1} ($= 10^{14}$ #polymer gels per L^{-1}) from Orellana et al. (2011). If the TEP particles in the
389 tropical atmosphere comprise only a small subgroup of the total polymer gel number, or if the
390 total amount of gel-like particles is generally higher in Polar Regions remains to be
391 investigated.

392 3.2 Relating atmospheric TEP to the ocean

393 From a recent study of TEP number concentrations in different oceanic regions, TEP
394 number concentrations in surface waters (10 m depth) of the East Tropical North Atlantic
395 (ETNA) were obtained (Engel et al., 2020). ETNA is the region that geographically includes the
396 Cape Verde islands. The oceanic TEP number concentrations are shown in **Fig. 5**. The TEP in
397 the ocean showed a similar size distribution compared to the TEP in the atmosphere (i.e.
398 aerosol particles and cloud water, **Fig. 4**) with increasing TEP number concentrations toward
399 smaller particle sizes (**Tab. S5** and more details in Engel et al. (2020)).

400

401 *Insert Fig. 5*

402

403 A detailed comparison of #TEP in the ocean and in the atmosphere regarding the
404 identical size bins showed that the #TEP distribution among the different size bins were much
405 more balanced for seawater than for aerosol particles. In aerosol particles, on average 51% of
406 the #TEP were located in the smallest analysed size bin (4.5-7 μm) and show a sharp decrease
407 towards the second size bin (that contained 24% of the TEP) (**Fig. 6**). For the seawater TEP,
408 however, around 35% of the #TEP were found in the first size bin and the relative contribution
409 decreased uniformly towards the larger size bins (**Fig. 6**). This distribution is also visible in the
410 correlation curves of **Fig 4 (b,d,f)** and **Figure 5b**. The correlation curves for the aerosol particles
411 (and cloud water) have a steeper slope compared to the curve obtained for seawater TEP. This
412 could imply that i) the transfer of TEP from the ocean to the atmosphere is most efficient for
413 small size ranges, ii) larger TEP are converted to smaller TEP in the atmosphere (e.g. break
414 down), and /or iii) atmospheric in-situ formation mechanism of TEP preferably occur in smaller
415 particle size ranges. These considerations will be further evaluated in section 3.3.

416

417 **Insert Figure 6**

418

419 To compare seawater and atmospheric TEP concentrations in terms of enrichment or
420 depletion, the atmospheric enrichment factor $EF_{atm.}$ (Equation 1) was calculated. However, the
421 TEP number concentrations in the ocean surface water were obtained from an additional
422 measurement campaign, taking place in the biologically productive Mauritanian Upwelling
423 region in the year 2012, hence at another time and season (Tab. 1). Compared to other oceanic
424 regions, the TEP values from the Mauritanian Upwelling region were at the higher end (Engel
425 et al., 2020). The region around the CVAO is rather oligotrophic and Chlorophyll-a values
426 during the MarParCloud campaign were relatively low with 0.1 up to 0.6 $\mu\text{g L}^{-1}$ (van Pinxteren
427 et al., 2020). As TEP production is often connected to phytoplankton activity, the TEP
428 concentration at the CVAO might be lower compared to more productive regions (Robinson
429 et al., 2019a). A previous study showed the total TEP number concentrations (covering TEP
430 sizes between 1 and 200 μm) at the Cape Verde islands (south of São Vicente at 16°44.4'N,
431 25°09.4'W) were by a factor of 2 lower than the data reported here, in detail $0.9 \times 10^7 \text{ L}^{-1}$ (Engel
432 et al., 2015) vs. $2 \times 10^7 \text{ L}^{-1}$ (Tab. S5). Lower TEP concentrations would result in higher $EF_{atm.}$
433 (Equation 1) regarding the ambient as well as the tank measurements as the same type of
434 seawater was used for the calculations. Hence, the here reported $EF_{atm.}$ represent lower limits.

435 In order to compare the same TEP diameters in all compartments, the size range
436 between 5 μm (lower limit for atmospheric measurements) and 10 μm (typical upper limit for
437 ambient aerosol particles) was regarded and converted from number to volume concentration
438 (more details in Table S2-S4 and Fig. S1). For ocean water, TEP number concentrations of
439 $3.5 \times 10^3 \text{ \#TEP mL}^{-1}$ ($= 3.5 \times 10^6 \text{ \#TEP L}^{-1}$) and a TEP volume concentration of $4.6 \times 10^5 \mu\text{m}^3 \text{ TEP mL}^{-1}$
440 ($= 3.5 \times 10^8 \mu\text{m}^3 \text{ TEP L}^{-1}$) were obtained. The respective values for the TEP volume
441 concentration of ambient and tank-generated aerosol particles, as well as for the cloud water
442 are listed in Tables S2-S4 and illustrated in **Fig 3b**. As mentioned above, the factors given here
443 are subject to some uncertainties and represent lower limits. An error discussion is introduced
444 in the Supporting Information as an appendix to Table S2. It is clearly visible that the $EF_{aer.}$
445 *ambient* are significantly higher than the $EF_{aer. tank}$ (ANOVA, oneway, $p = 0.0017$ at a 0.05 level)
446 with average values of 9×10^3 and 50, respectively. The average EF_{cloud} was 1×10^3 . This means
447 that the enrichment of TEP derived from the plunging waterfall tank, representing the bubble-
448 bursting transfer, is about two orders of magnitude lower compared to the enrichment of TEP
449 in the ambient aerosol particles.

450 It should be noted that the lower enrichment in the tank resulted from the lower TEP
451 number concentrations in the generated aerosol particles, as the particulate sodium
452 concentrations in the tank aerosol were even higher than in the ambient particles (Tab. S3).
453 This suggests that, although an artificial tank study cannot represent the ambient
454 environment, the generation of sea spray aerosol was in progress; however, TEP transfer
455 seemed to be not pronounced.

456 In the following, the here obtained enrichment factors will be discussed in more detail
457 considering studies available from literature.

458 Atmospheric enrichment of ocean-derived OM, have often been reported (e.g.
459 Facchini et al., 2008;Keene et al., 2007;O'Dowd et al., 2004;Schmitt-Kopplin et al.,
460 2012;Triesch et al., 2021a;Triesch et al., 2021b;van Pinxteren et al., 2017). Submicron particles
461 are usually strongly enriched with OM with aerosol enrichment factors $EF_{aer.}$ of 10^3 up to 10^5
462 (Quinn et al., 2015 and references therein). The enrichment in supermicron aerosol particles
463 is, however, significantly lower. Laboratory studies showed enrichment of OM in the order of
464 10^2 (Hoffman and Duce, 1976;Keene et al., 2007;Quinn et al., 2015). From the MarParCloud
465 campaign, enrichment factors of free amino acids were between 10 and 30 in ambient
466 supermicron particles (Triesch et al. 2021a). Kuznetsova et al. (2005) reported TEP
467 enrichments in freshly produced sea spray with $EF_{aer.} = 44 \pm 22$ based on TEP number
468 concentration. Consequently the here reported $EF_{aer. tank}$ (50 ± 35) are well in-line with
469 published enrichment factors for OM in general and TEP specifically. However, the $EF_{aer. ambient}$
470 (9×10^3) were orders of magnitude higher than reported enrichment factors for supermicron
471 aerosol particles. Enrichment factors of OM in cloud water are hardly available; we recently
472 reported an enrichment of $10^3 - 10^4$ of free amino acids in cloud water from the MarParCloud
473 campaign (Triesch et al., 2021a) that were higher than the here observed EF_{cloud} .

474 The concept of the aerosol enrichment factor originally originates from controlled tank
475 experiments where a direct transfer of compounds from the ocean via sea-spray aerosol
476 formation occurs. Obviously, this does not automatically correspond to the ambient
477 environment as mixing processes, aging, and further transformation reactions are not
478 accounted for. However, the $EF_{aer. ambient}$ which is much bigger than the $EF_{aer. tank}$ and the
479 comparison of EF_{cloud} towards former literature data clearly show the presence of significantly
480 more TEP in ambient aerosol and cloud water compared to oceanic seawater which will be
481 discussed in detail in the following section.

482

483 3.3 Possible sources and atmospheric formation pathways of TEP

484

485 3.3.1 Primary TEP sources

486

487 The high abundance of TEP in the aerosol particles and cloud water might correspond
488 to an oceanic transfer within the process of bubble bursting. To investigate a linkage to the
489 bubble bursting transfer, TEP concentrations were correlated to the wind speed, as well as to
490 the sea-spray tracers sodium and magnesium. To account for biases due to a number-based
491 (TEP) and mass-based (sodium, magnesium) comparison, the particle volume of TEP was
492 calculated from the particle number concentrations (regarding the size range: 5-10 μm). To
493 this end, from each particle diameter within a size range of 5-10 μm , the respective volume
494 was determined, assuming spherical particles, and summed up (data in **Tab. S2**). This

495 transformation accounts for the fact that big TEP particles likely possess a large mass but a
496 low number concentration and vice versa.

497 Reasonably good correlations of TEP to sodium, sea-salt calcium (Ca_{ss}) and magnesium,
498 ($R^2 = 0.5$, **Fig. 7a-c**) were found, suggested some connection to a bubble bursting transfer.
499 However, a correlation of TEP to wind speed was not found. It may be that since wind speed
500 data represented an average value of 24 hours, short but pronounced changes in the wind
501 speed were not visible in the average wind speed value. No correlation was found between
502 TEP and non-sea-salt calcium as well as total calcium (**Fig. 7d**).

503

504 ***Insert Figure 7***

505

506 Despite the correlation of TEP to sea spray tracers, the high abundance and enrichment
507 of #TEP in the ambient aerosol particles compared to literature data and compared to the
508 concentration and enrichment of the #TEP from the plunging waterfall tank performed here,
509 suggests that additional (secondary) TEP sources in the ambient atmosphere exist from which
510 TEPs are added to their primary transfer by bubble bursting from the oceans. At the Cape
511 Verde islands, besides the ocean, mineral dust is an important aerosol particle source (Fomba
512 et al., 2014). TEP are generally attributed to be ocean-derived compounds however, dust has
513 often been reported to transport attached biological particles (Maki et al., 2019; Marone et
514 al., 2020). During the MarParCloud campaign, dust influences were low to moderate and the
515 aerosol particle mass was found to be predominantly of marine origin (Fomba et al., 2014; van
516 Pinxteren et al., 2020). Some dust influences were visible though, e.g. variations in the particle
517 number concentrations, with elevated concentrations on (even low) dust influenced air
518 masses (Gong et al., 2020b). TEP number concentrations showed no clear connection to the
519 ambient dust concentrations (**Fig. 2**). Within periods of moderate dust, TEP were partly below
520 the detection limits (on 26.09.2017) and partly exhibited high concentrations (e.g. on 28. and
521 29.09.2017). A correlation between TEP and dust was not found ($R^2 = 0.05$, **Fig. 7e**) therefore,
522 we do not consider dust to be a transport medium for TEP to the particles or cloud water.
523 However, dust might play a role in abiotic TEP formation, as discussed in chapter 3.3.2.1.

524

525 3.3.2. In-situ formation

526

527 3.3.2.1 Abiotic formation

528

529 In aquatic environments, abiotic TEP formation has been reported to happen via
530 several pathways, including spontaneous assembly from TEP precursors (Passow, 2002b). The
531 aerosol particle and cloud water samples from the MarParCloud campaign investigated here
532 showed high mass concentrations of amino acids (up to 6.3 ng m^{-3} in the submicron aerosol
533 particles and up to 490 ng m^{-3} in the cloud water, published in Triesch et al. (2021a)) as well
534 as dissolved polysaccharides (up to 2 ng m^{-3} in the submicron aerosol particles and up to 2400

535 ng m⁻³ in the cloud water, results in preparation for publication). In the ocean, the dissolved
536 polysaccharides are known TEP precursors (Passow, 2002b) and Wurl et al. (2011) determined
537 abiotic TEP formation rates from dissolved polysaccharide concentration in various oceans.
538 The rates were on average $7.9 \pm 5.0 \mu\text{mol C L}^{-1} \text{ d}^{-1}$ and therefore significant considering that
539 the average TEP concentration was $18.1 \pm 15.9 \mu\text{mol C L}^{-1}$ and the average dissolved
540 polysaccharide concentration was $12.2 \pm 3.8 \mu\text{mol C L}^{-1}$ in the surface seawater (Wurl et al.,
541 2011). Robinson et al. (2019b) showed that rising bubbles can lead to an enhanced TEP
542 formation already after some minutes. The lifetime of supermicron aerosol particles, to which
543 the TEP particles studied here belong, are between hours and days, for example, Madry et al.
544 (2011) calculated an average lifetime of supermicron sea salt particles of 50 hours. Hence
545 abiotic TEP formation processes lie within the lifetime of supermicron aerosol particles and
546 we suggest that spontaneous TEP formation from the (high) abundant dissolved
547 polysaccharides likely contributed to the high TEP concentrations observed in the ambient
548 atmosphere in the present study. However, it needs to be considered that the abiotic TEP
549 formation processes described by Wurl et al. (2011) and Robinson et al. (2019b) were relevant
550 for the oceanic environment and might not directly translated to atmospheric processes.
551 Further studies are required on this topic.

552 Another important parameter likely impacting TEP formation is the presence of
553 mineral dust. As already discussed above, dust mass concentrations were low to moderate,
554 however not negligible, during the MarParCloud campaign. In laboratory minicosm studies,
555 the addition of dust to oceanic water resulted in an acceleration of the kinetics of TEP
556 formation leading to the formation of fast sinking particles (Louis et al., 2017). This process
557 likely happens due to particle aggregation, meaning that dissolved OM and dust aggregate to
558 form TEP (Louis et al., 2017). In addition, dust particles in cloud water might promote
559 turbulence, which, in aquatic media, has been suggested to enhance abiotic TEP formation
560 (Passow, 2002b). The dust deposition at the Cape Verdes has been recognized as a potentially
561 large contributing factor to the TEP enrichment in the SML at the Cape Verdes (Robinson et
562 al., 2019a). Here, we speculate that even low concentrations of mineral dust can influence the
563 TEP formation on the aerosol particles and in the cloud water. This is further supported by the
564 microscopic detection of dust in the cloud water (**Fig. 1**), that likely enhance the possibility
565 that particles in the cloud water collide and stick. Consequently, while dust did not seem to
566 serve as a transport medium for TEP (see sec. 3.3.1), dust may contribute to in-situ TEP
567 formation in cloud water due to abiotic particle aggregation.

568 From atmospheric studies, marine gel particles have been reported to undergo a
569 volume phase transition in response to environmental stimuli, such as pH and temperature as
570 well as cleavage of their polymers due to UV radiation (Orellana et al., 2011). UV radiation can
571 break down microgels in the ocean to a high number of smaller (nano-sized) particles (Orellana
572 and Verdugo, 2003) – a mechanism that is expected highly relevant in the atmosphere where
573 UV radiation is higher than in seawater. Furthermore, it has been shown that a lowering of
574 the pH from neutral conditions (7 or 8) to 4.5 causes a sudden transition of gel particles in

575 which the polymer network collapsed to a dense, non-porous array (Chin et al., 1998). As TEP
576 are reported to exhibit a gel-like character (Passow, 2002b), volume and number
577 concentrations might be affected by the different factors such as pH, ion density, temperature
578 and pressure in the atmosphere. The measured cloud water pH-value of the samples analysed
579 here was between 6.3 and 6.6, at which marine gels could split into smaller units (Chin et al.,
580 1998). Hence, a part of the cloud water TEP might be below the minimum detectable particle
581 size of 4.5 μm due to the slightly acidic conditions. This could explain the lower concentrations
582 in cloud water ($2 - 4 \times 10^3 \text{ \#TEP m}^{-3}$) compared to ambient aerosol particles ($7 \times 10^2 - 3 \times 10^4$
583 \#TEP m^{-3}). Hence, the different environmental stimuli likely impact atmospheric TEP formation
584 and might lead to the formation of smaller particles. However, from our data we cannot fully
585 explain the role of each of these effects and such investigations warrant further studies.

586 3.3.2.2 Biotic formation

587
588 Besides abiotic pathways, in aqueous media, TEP can be directly released as
589 particulates from aquatic organisms involving phytoplankton and bacteria (Passow, 2002a)
590 Biotic TEP formation has by now been studied for seawater and lakes (Passow, 2002a)
591 however, bacteria are also present in the atmosphere and likely transferred from the ocean
592 via sea spray (Rastelli et al., 2017) and can survive in cloud droplets (Deguillaume and al.,
593 2020). The bacterial abundance in cloud water samples taken at Mt. Verde during the
594 MarParCloud campaign ranged between 0.4 and $1.5 \times 10^5 \text{ cells mL}^{-1}$ (van Pinxteren et al., 2020).
595 This concentration is one to two orders of magnitude higher than the TEP concentrations. The
596 bacterial tracer muramic acid (Mimura and Romano, 1985) was detected in the aerosol
597 particles and cloud water sampled here in considerable concentrations ($\sim 25 \text{ nM}$, data not
598 shown), strongly suggesting bacterial activity in cloud water. We cannot derive conclusions on
599 the origin of the bacteria measured in cloud water reported here, however the transfer of
600 bacteria from the ocean to the atmosphere has been shown before (Rastelli et al.,
601 2017; Uetake et al., 2020). TEP are known to be closely connected to bacteria in different ways
602 (Passow, 2002b; Passow, 2002a), therefore, the presence of bacteria in the atmosphere
603 exhibits a potential source of cloud water TEP observed here. Furthermore, TEP are strongly
604 colonized by bacteria (Busch et al., 2017; Zäncker et al., 2019). Hence, TEP can be a transfer
605 vector for bacteria from the ocean to the atmosphere and/or act as a medium for bacterial
606 colonisation in marine clouds.

607 The presence of active enzymes on ambient aerosol particles (enriched compared to
608 seawater) and therefore biogenic in-situ cycling of OM through enzymatic reactions in
609 atmospheric particles was recently suggested (Malfatti et al., 2019). This is well in-line with
610 the findings that the aerosol particles and cloud water from the MarParCloud campaign
611 contained high concentrations of OM (amino acids, lipids), assumingly connected to a biogenic
612 formation (Triesch et al., 2021a; Triesch et al., 2021b). A combined approach of laboratory
613 experiments and modelling recently underlined the importance of biotic (and abiotic)
614 formation processes of OM in clouds (Jaber et al., 2021).

615 Regarding time scales of biotic processing, Matulova et al. (2014) showed that the
616 *Bacillus* sp. 3B6 isolated from cloud water was able to bio-transform saccharides that are
617 present in the atmosphere. The saccharides formed exopolymer substances (EPS), of which
618 TEP are a subgroup. The formation of EPS was revealed after 48 h of incubation and therefore
619 within the lifetime of supermicron aerosol particles (Madry et al., 2011).

620 Considering recent literature and the data reported here, we suggest that in-situ TEP
621 formation related to biogenic processes and likely connected to bacteria, as reported for
622 seawater, are important in the marine atmosphere as well. Besides, although not measured
623 here, microalgae and cyanobacteria, that are relevant for direct TEP formation in seawater,
624 have been reported to occur in the atmosphere (e.g. Lewandowska et al., 2017; Sharma et al.,
625 2007; Wiśniewska et al., 2019; Wiśniewska et al., 2022). It is worth studying, if these species
626 and their metabolic degradation products contribute to atmospheric TEP processing.

627

628 3.4 Connecting TEP and Ice nucleating particles (INP)

629 Different kinds of ice-nucleating macromolecules have been found in a certain range
630 of biological species and consist of a variety of chemical structures including proteins,
631 polysaccharides (Pummer et al., 2015) and lipids (DeMott et al., 2018). TEP, consisting of
632 polysaccharidic chains bridged with divalent cations, may therefore possess good properties
633 to act as INP, however, such a link has not yet been shown in field experiments.

634 During the MarParCloud campaign INP number concentration (N_{INP}) was measured in
635 different marine compartments and the results are presented in Gong et al. (2020a). By
636 combining INP concentration in the seawater, aerosol particles and cloud water, it was found
637 that N_{INP} in the atmosphere were at least four orders of magnitude higher than what would
638 be expected if all airborne INP would originate from sea spray. The measurements indicated
639 that other sources besides the ocean, such as mineral dust or other long-ranged transported
640 particles, contributed to the local INP concentration. However, some indications for
641 contributions of biological particles to the INP population were obtained (details in Gong et
642 al., 2020a). Nevertheless, the sources of INP could not be revealed in detail.

643 In the present study, quantitative INP data (presented in Gong et al. 2020a) and TEP
644 data measured from the same campaign were compared. To this end, INP concentrations
645 achieved from PM₁₀ quartz-fiber filters taken at the CVAO during the same period as the TSP
646 filters were compared with the TEP measurements. In addition, cloud water INP and TEP data
647 obtained from the same samples were combined.

648 TEP number concentrations were on average between $10^3 - 10^4 \text{ m}^{-3}$ in the ambient
649 aerosol particles, whereas INP number concentrations at $-15 \text{ }^\circ\text{C}$ were between $10 - 10^2 \text{ m}^{-3}$
650 (Gong et al., 2020a). It is interesting to note that the TEP concentrations in the ambient aerosol
651 particles were about two orders of magnitude higher compared to INP concentrations. Similar
652 findings were obtained for the cloud water comparisons; TEP concentrations ($\sim 10^6 \text{ L}^{-1}$) were

653 on average two orders of magnitude higher than INP number concentrations at -15 °C in cloud
654 water ($\sim 10^4 \text{ L}^{-1}$) (Gong et al., 2020a).

655 The correlation between INP (active at -15°C) and TEP concentrations was weak with
656 $R^2 = 0.3$ (**Fig. 7f**), showing that a direct link between INP and the entire TEP number
657 concentrations was not very pronounced. It needs to be underlined that TEP concentrations
658 below a particle size of 4.5 μm are not included here and according to the size distribution,
659 the TEP concentrations are increasing towards smaller sizes. Most of the here reported TEP
660 particles were in the supermicron size range between $\sim 4.5 - 14 \mu\text{m}$ (**Fig. 4**). However, the
661 biologically active N_{INP} at the Cape Verdes were mainly present in the supermicron mode (> 1
662 μm) (Gong et al., 2020a), hence a comparison with the TEP particle concentrations above 5
663 μm seems justified. Nevertheless, future studies should concentrate on the exact same size
664 ranges for TEP and INP.

665 The INP functionalities of biomolecules are not straightforward and whether a
666 macromolecule acts as INP is depending on many factors, as its size, proper position of
667 functional groups, and their allocation (Pummer et al., 2015). Typically, not the entire surface
668 of an INP but rather specific areas (active sites) participate in ice nucleation. This means that
669 despite TEP likely providing INP properties, only a fraction of TEP, if any, might be able to act
670 as INP. This hypothesis is supported by the findings that marine gels exhibit hydrophobic and
671 hydrophilic surface-active segments, strongly suggesting a dichotomous, non-uniform
672 behaviour of polymer gels (Leck et al., 2013; Orellana et al., 2011; Ovadnevaite et al., 2011). As
673 mentioned in 3.3.2.1 and 3.3.2.2, TEP are often attached to, or colonized with bacteria.
674 Bacteria itself, have been shown to provide excellent INP functionalities (Pandey et al., 2016)
675 and TEP might act as a carrying medium for INP, such as bacteria. Bacteria concentrations
676 were higher than TEP concentrations and also higher than INP concentrations. However, only
677 a fraction of all bacteria (0.5 – 25%) is associated with TEP and, vice versa, not all TEP are
678 colonized by bacteria (Passow, 2002b). There is an indication that especially in oligotrophic
679 waters, as are the Cape Verde islands, the fraction of bacteria attached to TEP is comparably
680 low (Schuster and Herndl, 1995). Hence, the concentration range of bacteria-colonized TEP in
681 relation to INP is worth further consideration. This might help to unravel if a functional
682 relationship between bacteria-colonized TEP and INP exists and if a certain part of TEP contain
683 fragments in the biological INP population that, beyond dust, play a role in the Cape Verde
684 atmosphere.

685

686 4 Conclusion

687

688 This study presented TEP number concentrations $> 4.5 \mu\text{m}$ in ambient atmospheric samples
689 from the tropical Atlantic Ocean during the MarParCloud campaign as well as in generated
690 atmospheric particles using a plunging waterfall tank. The atmospheric TEP showed a similar
691 size distribution compared to the TEP in the ocean with increasing TEP number concentrations
692 toward smaller particle sizes, however the #TEP distribution among the different size bins

693 were much more balanced for seawater than for aerosol particles where half of the #TEP were
694 located in the smallest analysed size bin (4.5-7 μm). Based on Na^+ concentrations in seawater
695 and the atmosphere, the enrichment of TEP in the tank generated aerosol particles was well
696 in-line with another study. The TEP enrichments in the ambient atmosphere were, however,
697 up to two orders of magnitude higher compared to the tank study and such high values are
698 thus far not reported for supermicron aerosol particles. We speculate that the high
699 enrichment of TEP in the particles and in cloud water result from a combination of enrichment
700 during bubble-bursting transfer from the ocean and secondary in-situ atmospheric formation.
701 We propose that similar (biotic and abiotic) formation mechanism reported for TEP formation
702 in the (sea)water might take place in the atmosphere as well, as the required conditions (e.g.
703 high concentrations of dissolved TEP precursors such as polysaccharides, presence of bacteria
704 in the cloud water) were given. An assessment of the importance of the biotic versus the
705 abiotic TEP formation pathways in the atmosphere, however, needs further investigations.
706 TEP concentrations in the atmosphere were two orders of magnitude higher than INP
707 concentrations in the aerosol particles and cloud water, respectively. However, only a part of
708 the TEP population, assumingly the one colonized by bacteria, might contribute to INP
709 population, and are worth further studies. Finally, while dust might be a dominant INP source
710 in the here investigated tropical Atlantic region close to the Saharan desert, in other remote
711 oceanic locations, marine gel particles, their in-cloud formation and connection to bacteria
712 and phytoplankton in the atmosphere could be highly relevant for a better understanding of
713 marine cloud properties.

714

715 Data availability

716 The TEP data are accessible under the following link
717 <https://doi.pangaea.de/10.1594/PANGAEA.938169>. INP concentrations are accessible under
718 the following link: <https://doi.pangaea.de/10.1594/PANGAEA.906946>.

719 Special issue statement

720 Acknowledgement

721 We acknowledge the funding by the Leibniz Association SAW in the project “Marine biological
722 production, organic aerosol particles and marine clouds: a Process Chain (MarParCloud)”
723 (SAW-2016-TROPOS-2), the Research and Innovation Staff Exchange EU project MARSU
724 (69089) and the Deutsche Forschungsgemeinschaft (DFG, German Research Foundation) –
725 Projektnummer 268020496 – TRR 172, within the Transregional Collaborative Research
726 Center “Arctic Amplification: Climate Relevant Atmospheric and Surface Processes, and
727 Feedback Mechanisms (AC)³” in sub-projects B04. We thank the CVAO site manager Luis Neves
728 as well as René Rabe and Susanne Fuchs for technical and laboratory assistance. We further
729 acknowledge the professional support provided by the Ocean Science Centre Mindelo (OSCM)
730 and the Instituto do Mar (IMar).

731

732 Author contributions

733 MvP led the MarParCloud campaign and, together with the campaign participants KWF, XG,
734 EB, NT, BR, FS and HW performed the aerosol particle and cloud water sampling at the Cape
735 Verde island. EB designed and operated the plunging waterfall tank. BR performed the
736 microscopic TEP measurements and XG made the INP analysis. AE contributed the seawater
737 TEP data. MvP performed the data interpretation with help from SZ and BR. MvP wrote the
738 manuscript with contributions from all authors.

739 Competing interest

740 The authors declare that they have no conflict of interest.

741

742 References

743 Alldredge, A. L., Passow, U., and Logan, B. E.: The abundance and significance of a class of
744 large, transparent organic particles in the ocean Deep-Sea Research Part I-Oceanographic Research
745 Papers, 40, 1131-1140, 10.1016/0967-0637(93)90129-q, 1993.

746 Aller, J. Y., Radway, J. C., Kilhau, W. P., Bothe, D. W., Wilson, T. W., Vaillancourt, R. D., Quinn,
747 P. K., Coffman, D. J., Murray, B. J., and Knopf, D. A.: Size-resolved characterization of the
748 polysaccharidic and proteinaceous components of sea spray aerosol, *Atmos. Environ.*, 154, 331-347,
749 10.1016/j.atmosenv.2017.01.053, 2017.

750 Bigg, E. K., and Leck, C.: The composition of fragments of bubbles bursting at the ocean
751 surface, *Journal of Geophysical Research-Atmospheres*, 113, 10.1029/2007jd009078, 2008.

752 Bittar, T. B., Passow, U., Hamaraty, L., Bidle, K. D., and Harvey, E. L.: An updated method for
753 the calibration of transparent exopolymer particle measurements, *Limnol. Oceanogr. Meth.*, 16, 621-
754 628, 10.1002/lom3.10268, 2018.

755 Blanchard, D. C.: Bubble Scavenging and the Water-to-Air Transfer of Organic Material in the
756 Sea, in: *Applied Chemistry at Protein Interfaces, Advances in Chemistry*, 145, American Chemical
757 Society, 360-387, 1975.

758 Burrows, S. M., Hoose, C., Poschl, U., and Lawrence, M. G.: Ice nuclei in marine air: biogenic
759 particles or dust?, *Atmospheric Chemistry and Physics*, 13, 245-267, 10.5194/acp-13-245-2013, 2013.

760 Busch, K., Endres, S., Iversen, M. H., Michels, J., Nothig, E. M., and Engel, A.: Bacterial
761 Colonization and Vertical Distribution of Marine Gel Particles (TEP and CSP) in the Arctic Fram Strait,
762 *Frontiers in Marine Science*, 4, 10.3389/fmars.2017.00166, 2017.

763 Carpenter, L. J., Fleming, Z. L., Read, K. A., Lee, J. D., Moller, S. J., Hopkins, J. R., Purvis, R. M.,
764 Lewis, A. C., Müller, K., Heinold, B., Herrmann, H., Fomba, K. W., van Pinxteren, D., Müller, C., Tegen,
765 I., Wiedensohler, A., Müller, T., Niedermeier, N., Achterberg, E. P., Patey, M. D., Kozlova, E. A.,
766 Heimann, M., Heard, D. E., Plane, J. M. C., Mahajan, A., Oetjen, H., Ingham, T., Stone, D., Whalley, L.

767 K., Evans, M. J., Pilling, M. J., Leigh, R. J., Monks, P. S., Karunaharan, A., Vaughan, S., Arnold, S. R.,
768 Tschirter, J., Pohler, D., Friess, U., Holla, R., Mendes, L. M., Lopez, H., Faria, B., Manning, A. J., and
769 Wallace, D. W. R.: Seasonal characteristics of tropical marine boundary layer air measured at the
770 Cape Verde Atmospheric Observatory, *Journal of Atmospheric Chemistry*, 67, 87-140,
771 10.1007/s10874-011-9206-1, 2010.

772 Chin, W. C., Orellana, M. V., and Verdugo, P.: Spontaneous assembly of marine dissolved
773 organic matter into polymer gels, *Nature*, 391, 568-572, 10.1038/35345, 1998.

774 Creamean, J. M., Cross, J. N., Pickart, R., McRaven, L., Lin, P., Pacini, A., Hanlon, R., Schmale, D.
775 G., Cenicerros, J., Aydell, T., Colombi, N., Bolger, E., and DeMott, P. J.: Ice Nucleating Particles Carried
776 From Below a Phytoplankton Bloom to the Arctic Atmosphere, *Geophysical Research Letters*, 46,
777 8572-8581, 10.1029/2019gl083039, 2019.

778 de Leeuw, G., Andreas, E. L., Anguelova, M. D., Fairall, C. W., Lewis, E. R., O'Dowd, C., Schulz,
779 M., and Schwartz, S. E.: Production Flux of Sea Spray Aerosol, *Reviews of Geophysics*, 49,
780 10.1029/2010rg000349, 2011.

781 Decho, A. W., and Gutierrez, T.: Microbial Extracellular Polymeric Substances (EPSs) in Ocean
782 Systems, *Frontiers in Microbiology*, 8, 10.3389/fmicb.2017.00922, 2017.

783 Deguillaume, L., and al., e.: Biological Activity in Clouds: From the Laboratory to the Model, in:
784 Air Pollution Modeling and its Application XXVI. ITM 2018., edited by: Mensink C., G. W., Hakami A. ,
785 pringer Proceedings in Complexity. Springer, Cham, 2020.

786 DeMott, P. J., Mason, R. H., McCluskey, C. S., Hill, T. C. J., Perkins, R. J., Desyaterik, Y., Bertram,
787 A. K., Trueblood, J. V., Grassian, V. H., Qiu, Y. Q., Molinero, V., Tobo, Y., Sultana, C. M., Lee, C., and
788 Prather, K. A.: Ice nucleation by particles containing long-chain fatty acids of relevance to freezing by
789 sea spray aerosols, *Environmental Science-Processes & Impacts*, 20, 1559-1569,
790 10.1039/c8em00386f, 2018.

791 Demoz, B. B., Collett, J. L., and Daube, B. C.: On the Caltech Active Strand Cloudwater
792 Collectors, *Atmos Res*, 41, 47-62, Doi 10.1016/0169-8095(95)00044-5, 1996.

793 Engel, A., Goldthwait, S., Passow, U., and Alldredge, A.: Temporal decoupling of carbon and
794 nitrogen dynamics in a mesocosm diatom bloom, *Limnology and Oceanography*, 47, 753-761,
795 10.4319/lo.2002.47.3.0753, 2002.

796 Engel, A., Delille, B., Jacquet, S., Riebesell, U., Rochelle-Newall, E., Terbruggen, A., and
797 Zondervan, I.: Transparent exopolymer particles and dissolved organic carbon production by
798 *Emiliana huxleyi* exposed to different CO₂ concentrations: a mesocosm experiment, *Aquatic*
799 *Microbial Ecology*, 34, 93-104, 10.3354/ame034093, 2004.

800 Engel, A.: Determination of Marine Gel Particles in: Practical guidelines for the analysis of
801 seawater, edited by: [u.a.], O. W. B. R., CRC Press, 2009.

802 Engel, A., Borchard, C., Loginova, A., Meyer, J., Hauss, H., and Kiko, R.: Effects of varied nitrate
803 and phosphate supply on polysaccharidic and proteinaceous gel particle production during tropical
804 phytoplankton bloom experiments, *Biogeosciences*, 12, 5647-5665, 10.5194/bg-12-5647-2015, 2015.

805 Engel, A., Endres, S., Galgani, L., and Schartau, M.: Marvelous Marine Microgels: On the
806 Distribution and Impact of Gel-Like Particles in the Oceanic Water-Column, *Frontiers in Marine*
807 *Science*, 7, 10.3389/fmars.2020.00405, 2020.

808 Ervens, B., and Amato, P.: The global impact of bacterial processes on carbon mass,
809 *Atmospheric Chemistry and Physics*, 20, 1777-1794, 10.5194/acp-20-1777-2020, 2020.

810 Facchini, M. C., Rinaldi, M., Decesari, S., Carbone, C., Finessi, E., Mircea, M., Fuzzi, S., Ceburnis,
811 D., Flanagan, R., Nilsson, E. D., de Leeuw, G., Martino, M., Woeltjen, J., and O'Dowd, C. D.: Primary
812 submicron marine aerosol dominated by insoluble organic colloids and aggregates, *Geophysical*
813 *Research Letters*, 35, 10.1029/2008gl034210, 2008.

814 Fomba, K. W., Müller, K., van Pinxteren, D., and Herrmann, H.: Aerosol size-resolved trace
815 metal composition in remote northern tropical Atlantic marine environment: case study Cape Verde
816 islands, *Atmospheric Chemistry and Physics*, 13, 4801-4814, 10.5194/acp-13-4801-2013, 2013.

817 Fomba, K. W., Mueller, K., van Pinxteren, D., Poulain, L., van Pinxteren, M., and Herrmann, H.:
818 Long-term chemical characterization of tropical and marine aerosols at the Cape Verde Atmospheric
819 Observatory (CVAO) from 2007 to 2011, *Atmospheric Chemistry and Physics*, 14, 8883-8904,
820 10.5194/acp-14-8883-2014, 2014.

821 Gao, Q., Leck, C., Rauschenberg, C., and Matrai, P. A.: On the chemical dynamics of
822 extracellular polysaccharides in the high Arctic surface microlayer, *Ocean Sci.*, 8, 401-418,
823 10.5194/os-8-401-2012, 2012.

824 Gong, X. D., Wex, H., van Pinxteren, M., Triesch, N., Fomba, K. W., Lubitz, J., Stolle, C.,
825 Robinson, T. B., Muller, T., Herrmann, H., and Stratmann, F.: Characterization of aerosol particles at
826 Cabo Verde close to sea level and at the cloud level - Part 2: Ice-nucleating particles in air, cloud and
827 seawater, *Atmospheric Chemistry and Physics*, 20, 1451-1468, 10.5194/acp-20-1451-2020, 2020a.

828 Gong, X. D., Wex, H., Voigtlander, J., Fomba, K. W., Weinhold, K., van Pinxteren, M., Henning,
829 S., Muller, T., Herrmann, H., and Stratmann, F.: Characterization of aerosol particles at Cabo Verde
830 close to sea level and at the cloud level - Part 1: Particle number size distribution, cloud condensation
831 nuclei and their origins, *Atmospheric Chemistry and Physics*, 20, 1431-1449, 10.5194/acp-20-1431-
832 2020, 2020b.

833 Hartmann, M., Adachi, K., Eppers, O., Haas, C., Herber, A., Holzinger, R., Hunerbein, A., Jakel,
834 E., Jentzsch, C., van Pinxteren, M., Wex, H., Willmes, S., and Stratmann, F.: Wintertime Airborne
835 Measurements of Ice Nucleating Particles in the High Arctic: A Hint to a Marine, Biogenic Source for
836 Ice Nucleating Particles, *Geophysical Research Letters*, 47, 10.1029/2020gl087770, 2020.

837 Hoffman, E. J., and Duce, R. A.: Factors influencing organic-carbon content of marine aerosols -
838 Laboratory study, *J. Geophys. Res.*, 81, 3667-3670, 1976.

839 Jaber, S., Joly, M., Brissy, M., Lereboure, M., Khaled, A., Ervens, B., and Delort, A. M.: Biotic
840 and abiotic transformation of amino acids in cloud water: experimental studies and atmospheric
841 implications, *Biogeosciences*, 18, 1067-1080, 10.5194/bg-18-1067-2021, 2021.

842 Keene, W. C., Maring, H., Maben, J. R., Kieber, D. J., Pszenny, A. A. P., Dahl, E. E., Izaguirre, M.
843 A., Davis, A. J., Long, M. S., Zhou, X., Smoydzin, L., and Sander, R.: Chemical and physical
844 characteristics of nascent aerosols produced by bursting bubbles at a model air-sea interface, *Journal*
845 *of Geophysical Research-Atmospheres*, 112, 10.1029/2007jd008464, 2007.

846 Khaled, A., Zhang, M. H., Amato, P., Delort, A. M., and Ervens, B.: Biodegradation by bacteria in
847 clouds: an underestimated sink for some organics in the atmospheric multiphase system,
848 *Atmospheric Chemistry and Physics*, 21, 3123-3141, 10.5194/acp-21-3123-2021, 2021.

849 Kuznetsova, M., Lee, C., and Aller, J.: Characterization of the proteinaceous matter in marine
850 aerosols, *Marine Chemistry*, 96, 359-377, 10.1016/j.marchem.2005.03.007, 2005.

851 Leck, C., and Bigg, E. K.: Source and evolution of the marine aerosol - A new perspective,
852 *Geophysical Research Letters*, 32, 10.1029/2005gl023651, 2005a.

853 Leck, C., and Bigg, E. K.: Biogenic particles in the surface microlayer and overlying atmosphere
854 in the central Arctic Ocean during summer, *Tellus Ser. B-Chem. Phys. Meteorol.*, 57, 305-316,
855 10.1111/j.1600-0889.2005.00148.x, 2005b.

856 Leck, C., Gao, Q., Rad, F. M., and Nilsson, U.: Size-resolved atmospheric particulate
857 polysaccharides in the high summer Arctic, *Atmospheric Chemistry and Physics*, 13, 12573-12588,
858 10.5194/acp-13-12573-2013, 2013.

859 Lewandowska, A. U., and Falkowska, L. M.: Sea salt in aerosols over the southern Baltic. Part 1.
860 The generation and transportation of marine particles, *Oceanologia*, 55, 279-298, 10.5697/oc.55-
861 2.279, 2013.

862 Lewandowska, A. U., Sliwinska-Wilczewska, S., and Wozniczka, D.: Identification of
863 cyanobacteria and microalgae in aerosols of various sizes in the air over the Southern Baltic Sea,
864 *Marine Pollution Bulletin*, 125, 30-38, 10.1016/j.marpolbul.2017.07.064, 2017.

865 Liss, P. S., and Johnson, M. T.: *Ocean-Atmosphere Interactions of Gases and Particles*, Springer,
866 2014.

867 Logan, B. E., Passow, U., Alldredge, A. L., Grossartt, H.-P., and Simont, M.: Rapid formation and
868 sedimentation of large aggregates is predictable from coagulation rates (half-lives) of transparent
869 exopolymer particles (TEP), *Deep Sea Research Part II: Topical Studies in Oceanography*, 42, 203-214,
870 [https://doi.org/10.1016/0967-0645\(95\)00012-F](https://doi.org/10.1016/0967-0645(95)00012-F), 1995.

871 Louis, J., Pedrotti, M. L., Gazeau, F., and Guieu, C.: Experimental evidence of formation of
872 Transparent Exopolymer Particles (TEP) and POC export provoked by dust addition under current and
873 high pCO₂ conditions, *Plos One*, 12, 10.1371/journal.pone.0171980, 2017.

874 Madry, W. L., Toon, O. B., and O'Dowd, C. D.: Modeled optical thickness of sea-salt aerosol,
875 *Journal of Geophysical Research-Atmospheres*, 116, 10.1029/2010jd014691, 2011.

876 Maki, T., Lee, K. C., Kawai, K., Onishi, K., Hong, C. S., Kurosaki, Y., Shinoda, M., Kai, K., Iwasaka,
877 Y., Archer, S. D. J., Lacap-Bugler, D. C., Hasegawa, H., and Pointing, S. B.: Aeolian Dispersal of Bacteria
878 Associated With Desert Dust and Anthropogenic Particles Over Continental and Oceanic Surfaces,
879 *Journal of Geophysical Research-Atmospheres*, 124, 5579-5588, 10.1029/2018jd029597, 2019.

880 Malfatti, F., Lee, C., Tinta, T., Pendergraft, M. A., Celussi, M., Zhou, Y. Y., Sultana, C. M., Rotter,
881 A., Axson, J. L., Collins, D. B., Santander, M. V., Morales, A. L. A., Aluwihare, L. I., Riemer, N., Grassian,
882 V. H., Azam, F., and Prather, K. A.: Detection of Active Microbial Enzymes in Nascent Sea Spray
883 Aerosol: Implications for Atmospheric Chemistry and Climate, *Environmental Science & Technology*
884 *Letters*, 6, 171-177, 10.1021/acs.estlett.8b00699, 2019.

885 Mari, X., Passow, U., Migon, C., Burd, A. B., and Legendre, L.: Transparent exopolymer
886 particles: Effects on carbon cycling in the ocean, *Progress in Oceanography*, 151, 13-37,
887 10.1016/j.pocean.2016.11.002, 2017.

888 Marone, A., Kane, C. T., Mbengue, M., Jenkins, G. S., Niang, D. N., Drame, M. S., and Gernand,
889 J. M.: Characterization of Bacteria on Aerosols From Dust Events in Dakar, Senegal, West Africa,
890 *Geohealth*, 4, 10.1029/2019gh000216, 2020.

891 Matulova, M., Husarova, S., Capek, P., Sancelme, M., and Delort, A. M.: Biotransformation of
892 Various Saccharides and Production of Exopolymeric Substances by Cloud-Borne *Bacillus* sp 3B6,
893 *Environmental Science & Technology*, 48, 14238-14247, 10.1021/es501350s, 2014.

894 McCluskey, C. S., Hill, T. C. J., Humphries, R. S., Rauker, A. M., Moreau, S., Strutton, P. G.,
895 Chambers, S. D., Williams, A. G., McRobert, I., Ward, J., Keywood, M. D., Harnwell, J., Ponsonby, W.,
896 Loh, Z. M., Krummel, P. B., Protat, A., Kreidenweis, S. M., and DeMott, P. J.: Observations of Ice
897 Nucleating Particles Over Southern Ocean Waters, *Geophysical Research Letters*, 45, 11989-11997,
898 10.1029/2018gl079981, 2018a.

899 McCluskey, C. S., Ovadnevaite, J., Rinaldi, M., Atkinson, J., Belosi, F., Ceburnis, D., Marullo, S.,
900 Hill, T. C. J., Lohmann, U., Kanji, Z. A., O'Dowd, C., Kreidenweis, S. M., and DeMott, P. J.: Marine and
901 Terrestrial Organic Ice-Nucleating Particles in Pristine Marine to Continentally Influenced Northeast
902 Atlantic Air Masses, *Journal of Geophysical Research-Atmospheres*, 123, 6196-6212,
903 10.1029/2017jd028033, 2018b.

904 Mimura, T., and Romano, J. C.: Muramin acid measurements for bacterial investigations in
905 marine environments by high-pressure-liquid-chromatography, *Applied and Environmental*
906 *Microbiology*, 50, 229-237, 10.1128/aem.50.2.229-237.1985, 1985.

907 Niedermeier, N., Held, A., Müller, T., Heinold, B., Schepanski, K., Tegen, I., Kandler, K., Ebert,
908 M., Weinbruch, S., Read, K., Lee, J., Fomba, K. W., Müller, K., Herrmann, H., and Wiedensohler, A.:
909 Mass deposition fluxes of Saharan mineral dust to the tropical northeast Atlantic Ocean: an
910 intercomparison of methods, *Atmos. Chem. Phys.*, 14, 2245-2266, 10.5194/acp-14-2245-2014, 2014.

911 O'Dowd, C. D., Facchini, M. C., Cavalli, F., Ceburnis, D., Mircea, M., Decesari, S., Fuzzi, S., Yoon,
912 Y. J., and Putaud, J. P.: Biogenically driven organic contribution to marine aerosol, *Nature*, 431, 676-
913 680, Doi 10.1038/Nature02959, 2004.

914 Orellana, M. V., and Verdugo, P.: Ultraviolet radiation blocks the organic carbon exchange
915 between the dissolved phase and the gel phase in the ocean, *Limnology and Oceanography*, 48,
916 1618-1623, 10.4319/lo.2003.48.4.1618, 2003.

917 Orellana, M. V., Matrai, P. A., Leck, C., Rauschenberg, C. D., Lee, A. M., and Coz, E.: Marine
918 microgels as a source of cloud condensation nuclei in the high Arctic, *Proceedings of the National*
919 *Academy of Sciences of the United States of America*, 108, 13612-13617, 10.1073/pnas.1102457108,
920 2011.

921 Ovadnevaite, J., O'Dowd, C., Dall'Osto, M., Ceburnis, D., Worsnop, D. R., and Berresheim, H.:
922 Detecting high contributions of primary organic matter to marine aerosol: A case study, *Geophysical*
923 *Research Letters*, 38, 10.1029/2010gl046083, 2011.

924 Pandey, R., Usui, K., Livingstone, R. A., Fischer, S. A., Pfaendtner, J., Backus, E. H. G., Nagata, Y.,
925 Frohlich-Nowoisky, J., Schmuser, L., Mauri, S., Scheel, J. F., Knopf, D. A., Poschl, U., Bonn, M., and

- 926 Weidner, T.: Ice-nucleating bacteria control the order and dynamics of interfacial water, *Science*
 927 *Advances*, 2, 10.1126/sciadv.1501630, 2016.
- 928 Passow, U., and Alldredge, A.: A dye-binding assay for the spectrophotometric measurement of
 929 transparent exopolymer particles (TEP), *Limnology and Oceanography*, 40, 10, 1995.
- 930 Passow, U.: Formation of transparent exopolymer particles, TEP, from dissolved precursor
 931 material, *Marine Ecology Progress Series*, 192, 1-11, 10.3354/meps192001, 2000.
- 932 Passow, U.: Production of transparent exopolymer particles (TEP) by phyto- and
 933 bacterioplankton, *Marine Ecology-progress Series - MAR ECOL-PROGR SER*, 236, 1-12,
 934 10.3354/meps236001, 2002a.
- 935 Passow, U.: Transparent exopolymer particles (TEP) in aquatic environments, *Progress in*
 936 *Oceanography*, 55, 287-333, 10.1016/s0079-6611(02)00138-6, 2002b.
- 937 Pummer, B. G., Budke, C., Augustin-Bauditz, S., Niedermeier, D., Felgitsch, L., Kampf, C. J.,
 938 Huber, R. G., Liedl, K. R., Loerting, T., Moschen, T., Schauperl, M., Tollinger, M., Morris, C. E., Wex, H.,
 939 Grothe, H., Poschl, U., Koop, T., and Frohlich-Nowoisky, J.: Ice nucleation by water-soluble
 940 macromolecules, *Atmospheric Chemistry and Physics*, 15, 4077-4091, 10.5194/acp-15-4077-2015,
 941 2015.
- 942 Quinn, P. K., Collins, D. B., Grassian, V. H., Prather, K. A., and Bates, T. S.: Chemistry and
 943 Related Properties of Freshly Emitted Sea Spray Aerosol, *Chemical Reviews*, 115, 4383-4399,
 944 10.1021/cr5007139, 2015.
- 945 Rastelli, E., Corinaldesi, C., Dell'Anno, A., Lo Martire, M., Greco, S., Facchini, M. C., Rinaldi, M.,
 946 O'Dowd, C., Ceburnis, D., and Danovaro, R.: Transfer of labile organic matter and microbes from the
 947 ocean surface to the marine aerosol: an experimental approach, *Scientific Reports*, 7,
 948 10.1038/s41598-017-10563-z, 2017.
- 949 Robinson, T. B., Stolle, C., and Wurl, O.: Depth is relative: the importance of depth for
 950 transparent exopolymer particles in the near-surface environment, *Ocean Science*, 15, 1653-1666,
 951 10.5194/os-15-1653-2019, 2019a.
- 952 Robinson, T. B., Wurl, O., Bahlmann, E., Juergens, K., and Stolle, C.: Rising bubbles enhance the
 953 gelatinous nature of the air-sea interface, *Limnology and Oceanography*, 64, 2358-2372,
 954 10.1002/lno.11188, 2019b.
- 955 Sander, R., Keene, W. C., Pszenny, A. A. P., Arimoto, R., Ayers, G. P., Baboukas, E., Caine, J. M.,
 956 Crutzen, P. J., Duce, R. A., Honninger, G., Huebert, B. J., Maenhaut, W., Mihalopoulos, N., Turekian, V.
 957 C., and Van Dingenen, R.: Inorganic bromine in the marine boundary layer: a critical review,
 958 *Atmospheric Chemistry and Physics*, 3, 1301-1336, 2003.
- 959 Schmitt-Kopplin, P., Liger-Belair, G., Koch, B. P., Flerus, R., Kattner, G., Harir, M., Kanawati, B.,
 960 Lucio, M., Tziotis, D., Hertkorn, N., and Gebefuegi, I.: Dissolved organic matter in sea spray: a transfer
 961 study from marine surface water to aerosols, *Biogeosciences*, 9, 1571-1582, 10.5194/bg-9-1571-
 962 2012, 2012.
- 963 Schuster, S., and Herndl, G. J.: Formation and significance of transparent exopolymeric
 964 particles in the northern adriatic sea *Marine Ecology Progress Series*, 124, 227-236,
 965 10.3354/meps124227, 1995.

966 Sellegrì, K., Nicosia, A., Freney, E., Uitz, J., Thyssen, M., Grégori, G., Engel, A., Zäncker, B.,
967 Haëntjens, N., Mas, S., Picard, D., Saint-Macary, A., Peltola, M., Rose, C., Trueblood, J., Lefevre, D.,
968 D'Anna, B., Desboeufs, K., Meskhidze, N., Guieu, C., and Law, C. S.: Surface ocean microbiota
969 determine cloud precursors, *Scientific Reports*, 11, 281, 10.1038/s41598-020-78097-5, 2021.

970 Sharma, N. K., Rai, A. K., Singh, S., and Brown, R. M.: Airborne algae: Their present status and
971 relevance, *Journal of Phycology*, 43, 615-627, 10.1111/j.1529-8817.2007.00373.x, 2007.

972 Triesch, N., van Pinxteren, M., Engel, A., and Herrmann, H.: Concerted measurements of free
973 amino acids at the Cape Verde Islands: High enrichments in submicron sea spray aerosol particles
974 and cloud droplets, *Atmos. Chem. Phys.*, 21, 163–181, 2021a.

975 Triesch, N., van Pinxteren, M., Frka, S., Stolle, C., Spranger, T., Hoffmann, E. H., Gong, X., Wex,
976 H., Schulz-Bull, D., Gašparović, B., and Herrmann, H.: Concerted measurements of lipids in seawater
977 and on submicrometer aerosol particles at the Cabo Verde islands: biogenic sources, selective
978 transfer and high enrichments, *Atmos. Chem. Phys.*, 21, 4267-4283, 10.5194/acp-21-4267-2021,
979 2021b.

980 Turekian, K. K.: *Oceans (Foundations of Earth Science)*, Prentice Hall; 1st Edition, 1968.

981 Uetake, J., Hill, T. C. J., Moore, K. A., DeMott, P. J., Protat, A., and Kreidenweis, S. M.: Airborne
982 bacteria confirm the pristine nature of the Southern Ocean boundary layer, *Proceedings of the
983 National Academy of Sciences of the United States of America*, 117, 13275-13282,
984 10.1073/pnas.2000134117, 2020.

985 van Pinxteren, M., Barthel, S., Fomba, K., Müller, K., von Tümpling, W., and Herrmann, H.: The
986 influence of environmental drivers on the enrichment of organic carbon in the sea surface microlayer
987 and in submicron aerosol particles – measurements from the Atlantic Ocean, *Elem Sci Anth*, 5,
988 <https://doi.org/10.1525/elementa.225>, 2017.

989 van Pinxteren, M., Fomba, K. W., Triesch, N., Stolle, C., Wurl, O., Bahlmann, E., Gong, X. D.,
990 Voigtlander, J., Wex, H., Robinson, T. B., Barthel, S., Zeppenfeld, S., Hoffmann, E. H., Roveretto, M., Li,
991 C. L., Grosselin, B., Daele, V., Senf, F., van Pinxteren, D., Manzi, M., Zabalegui, N., Frka, S., Gasparovic,
992 B., Pereira, R., Li, T., Wen, L., Li, J. R., Zhu, C., Chen, H., Chen, J. M., Fiedler, B., Von Tümpling, W.,
993 Read, K. A., Punjabi, S., Lewis, A. C., Hopkins, J. R., Carpenter, L. J., Peeken, I., Rixen, T., Schulz-Bull,
994 D., Monge, M. E., Mellouki, A., George, C., Stratmann, F., and Herrmann, H.: Marine organic matter in
995 the remote environment of the Cape Verde islands - an introduction and overview to the
996 MarParCloud campaign, *Atmospheric Chemistry and Physics*, 20, 6921-6951, 10.5194/acp-20-6921-
997 2020, 2020.

998 Verdugo, P., Alldredge, A. L., Azam, F., Kirchman, D. L., Passow, U., and Santschi, P. H.: The
999 oceanic gel phase: a bridge in the DOM–POM continuum, *Marine Chemistry*, 92, 67-85, 2004.

1000 Villacorte, L. O., Ekowati, Y., Calix-Ponce, H. N., Schippers, J. C., Amy, G. L., and Kennedy, M. D.:
1001 Improved method for measuring transparent exopolymer particles (TEP) and their precursors in fresh
1002 and saline water, *Water Research*, 70, 300-312, 10.1016/j.watres.2014.12.012, 2015.

1003 Wiedensohler, A., Birmili, W., Nowak, A., Sonntag, A., Weinhold, K., Merkel, M., Wehner, B.,
1004 Tuch, T., Pfeifer, S., Fiebig, M., Fjaraa, A. M., Asmi, E., Sellegri, K., Depuy, R., Venzac, H., Villani, P., Laj,
1005 P., Aalto, P., Ogren, J. A., Swietlicki, E., Williams, P., Roldin, P., Quincey, P., Hüglin, C., Fierz-
1006 Schmidhauser, R., Gysel, M., Weingartner, E., Riccobono, F., Santos, S., Gruning, C., Faloon, K.,

1007 Beddows, D., Harrison, R. M., Monahan, C., Jennings, S. G., O'Dowd, C. D., Marinoni, A., Horn, H. G.,
1008 Keck, L., Jiang, J., Scheckman, J., McMurry, P. H., Deng, Z., Zhao, C. S., Moerman, M., Henzing, B., de
1009 Leeuw, G., Loschau, G., and Bastian, S.: Mobility particle size spectrometers: harmonization of
1010 technical standards and data structure to facilitate high quality long-term observations of
1011 atmospheric particle number size distributions, *Atmospheric Measurement Techniques*, 5, 657-685,
1012 10.5194/amt-5-657-2012, 2012.

1013 Wilson, T. W., Ladino, L. A., Alpert, P. A., Breckels, M. N., Brooks, I. M., Browse, J., Burrows, S.
1014 M., Carslaw, K. S., Huffman, J. A., Judd, C., Kiltthau, W. P., Mason, R. H., McFiggans, G., Miller, L. A.,
1015 Najera, J. J., Polishchuk, E., Rae, S., Schiller, C. L., Si, M., Temprado, J. V., Whale, T. F., Wong, J. P. S.,
1016 Wurl, O., Yakobi-Hancock, J. D., Abbatt, J. P. D., Aller, J. Y., Bertram, A. K., Knopf, D. A., and Murray, B.
1017 J.: A marine biogenic source of atmospheric ice-nucleating particles, *Nature*, 525, 234-+,
1018 10.1038/nature14986, 2015.

1019 Wiśniewska, K., Lewandowska, A. U., and Śliwińska-Wilczewska, S.: The importance of
1020 cyanobacteria and microalgae present in aerosols to human health and the environment - Review
1021 study, *Environment International*, 131, 10.1016/j.envint.2019.104964, 2019.

1022 Wiśniewska, K. A., Śliwińska-Wilczewska, S., and Lewandowska, A. U.: Airborne microalgal and
1023 cyanobacterial diversity and composition during rain events in the southern Baltic Sea region,
1024 *Scientific Reports*, 12, 2029, 10.1038/s41598-022-06107-9, 2022.

1025 Wurl, O., and Holmes, M.: The gelatinous nature of the sea-surface microlayer, *Marine*
1026 *Chemistry*, 110, 89-97, 10.1016/j.marchem.2008.02.009, 2008.

1027 Wurl, O., Miller, L., and Vagle, S.: Production and fate of transparent exopolymer particles in
1028 the ocean, *J. Geophys. Res.-Oceans*, 116, 10.1029/2011jc007342, 2011.

1029 Zäncker, B., Engel, A., and Cunliffe, M.: Bacterial communities associated with individual
1030 transparent exopolymer particles (TEP), *Journal of Plankton Research*, 41, 561-565,
1031 10.1093/plankt/fbz022, 2019.

1032 Zeppenfeld, S., van Pinxteren, M., Hartmann, M., Bracher, A., Stratmann, F., and Herrmann, H.:
1033 Glucose as a Potential Chemical Marker for Ice Nucleating Activity in Arctic Seawater and Melt Pond
1034 Samples, *Environmental Science & Technology*, 53, 8747-8756, 10.1021/acs.est.9b01469, 2019.

1035 Zeppenfeld, S., van Pinxteren, M., van Pinxteren, D., Wex, H., Berdalet, E., Vaqué, D., Dall'Osto,
1036 M., and Herrmann, H.: Aerosol Marine Primary Carbohydrates and Atmospheric Transformation in
1037 the Western Antarctic Peninsula, *ACS Earth Space Chem.*, 10.1021/acsearthspacechem.0c00351,
1038 2021.

1039 Zhang, M. H., Khaled, A., Amato, P., Delort, A. M., and Ervens, B.: Sensitivities to biological
1040 aerosol particle properties and ageing processes: potential implications for aerosol-cloud interactions
1041 and optical properties, *Atmospheric Chemistry and Physics*, 21, 3699-3724, 10.5194/acp-21-3699-
1042 2021, 2021.

1043

1044

1045

1046 **Caption of Figures:**

1047 **Figure 1:** Microscopic analysis of TEP from the cloud water sample “WW5” (sampling interval:
1048 28.09. 19:30 – 29.09. 7:30 local time). Blue particles are TEP, stained with Alcian Blue solution;
1049 brownish particles in the right picture are assumingly dust particles. The scale refers to 50 μm .
1050

1051 **Figure 2:** TEP number concentrations in the aerosol particles (red bars) and in the three cloud
1052 water samples (black-red squares). TEP concentrations were below the limit of detection
1053 (LOD) on 26th of September 2017. The backgrounds represent the dust classification
1054 according to the ambient dust concentrations (blue: dust < 5 $\mu\text{g m}^{-3}$ marine conditions; yellow:
1055 dust < 20 $\mu\text{g m}^{-3}$ (low dust); brown: dust < 60 $\mu\text{g m}^{-3}$ (moderate dust). From underlined dates
1056 (22.09 -> “TEP5” and 28.09.2017 -> “TEP10”) TEP number size distributions were measured.
1057

1058 **Figure 3:** Box and whisker plot of the TEP number concentrations (a) and the enrichment
1059 factors (b) in the ambient (n=18) and tank-generated (n=4) aerosol particles and in the cloud
1060 water samples (n=3), Each box encloses 50% of the data with the mean value represented as
1061 an open square and the median value represented as a line. The bottom of the box marks the
1062 25% limit of the data, while the top marks the 75% limit. The lines extending from the top and
1063 bottom of each box are the 5% and 95% percentiles within the data set, while the asterisks
1064 indicate the data points lying outside of this range (“outliers”).

1065 **Figure 4:** TEP number size distribution in the aerosol particles and cloud water in linear and
1066 logarithmic form; panels (a) and (b) show aerosol particle sample “TEP 5” (sampling start:
1067 22.09.2017), panels (c) and (d) show aerosol sample “TEP 10” (sampling start: 28.09.2017),
1068 panels (e) and (f) show cloud water sample “WW5” (sampling interval: 28.09. 19:30 – 29.09.
1069 7:30 local time. The lower limit of the resolution of the microscope was 16 μm^2 resulting in a
1070 particle diameter of 4.5 μm (assuming spherical particle). Each bar in a), c), and e) represents
1071 the summed up particle number concentrations (within 1.5 μm), e.g. the first column
1072 represents the summed up concentrations between 4.5 and 6 μm .
1073

1074 **Figure 5:** TEP number size distributions in the ocean surface water (sampling depth: 10 m)
1075 from the East Tropical North Atlantic (ETNA), averaged over three stations from Engel et al
1076 (2020). The data in this Figure show the size distribution between ~ 5 and ~ 30 μm , matching
1077 the investigated aerosol size range (**Fig. 4**). The whole size spectrum is shown in **Tab. S5**.
1078

1079 **Figure 6:** Relative contribution of the TEP number concentrations in the aerosol particles
1080 (left) and in the ocean surface water (right) regarding the identical size bins.

1081

1082 **Figure 7:** Correlations of TEP volume concentrations (size range: 5-10 μm) to chemical
1083 parameters (inorganic constituents PM10) and dust (PM10), as well as correlation of TEP
1084 number concentration and INP number concentrations. Inorganic constituents were
1085 measured with ion chromatography and dust concentrations were derived from PM10
1086 concentrations as reported elsewhere (Fomba et al., 2013;van Pinxteren et al., 2020).
1087 Measurements of INP number concentrations and error bars are explained in (Gong et al.,
1088 2020a)

1089
1090
1091
1092
1093
1094
1095
1096
1097
1098
1099
1100
1101
1102
1103
1104
1105
1106
1107
1108
1109
1110
1111
1112
1113
1114
1115
1116
1117
1118
1119
1120
1121
1122
1123
1124
1125
1126
1127

1128

1129 Table 1. Overview of sampling locations, types and measurements

Sampling site	Campaign	Sample type	Coordinates	No. of samples	Measurements (Particle sizes)
CVAO	MarParCloud 2017	Ambient aerosol particles Inlet high: 42 m a.s.l	16° 51.49' N, 24° 52.02' W	20 20	#TEP (TSP) Inorganic ions (PM ₁₀)
Mt- Verde	MarParCloud 2017	Ambient cloud water Inlet high: 746 m a.s.l	16°52.11'N, 24°56.02'W	3	#TEP Inorganic ions
Plunging waterfall tank (operated at CVAO)	MarParCloud 2017	Tank-generated aerosol particles	16° 51.49' N, 24° 52.02' W	4	#TEP (TSP) Inorganic ions (TSP)
ETNA (Mauretanian upwelling)	M107 RV Meteor 2012	Ocean surface water	18.00/18.19'N -16.50/72.02'E	6	#TEP

1130

1131

1132

1133

1134

1135
1136
1137
1138
1139
1140
1141
1142
1143
1144
1145
1146
1147
1148
1149
1150
1151
1152
1153

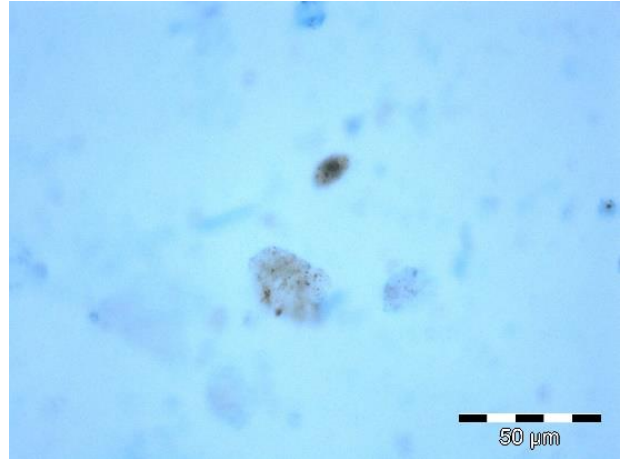
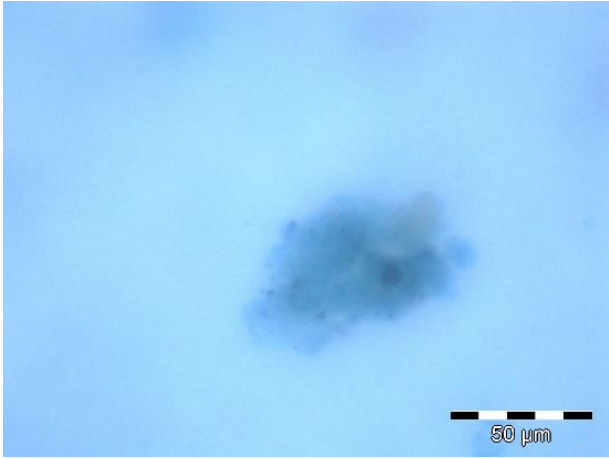
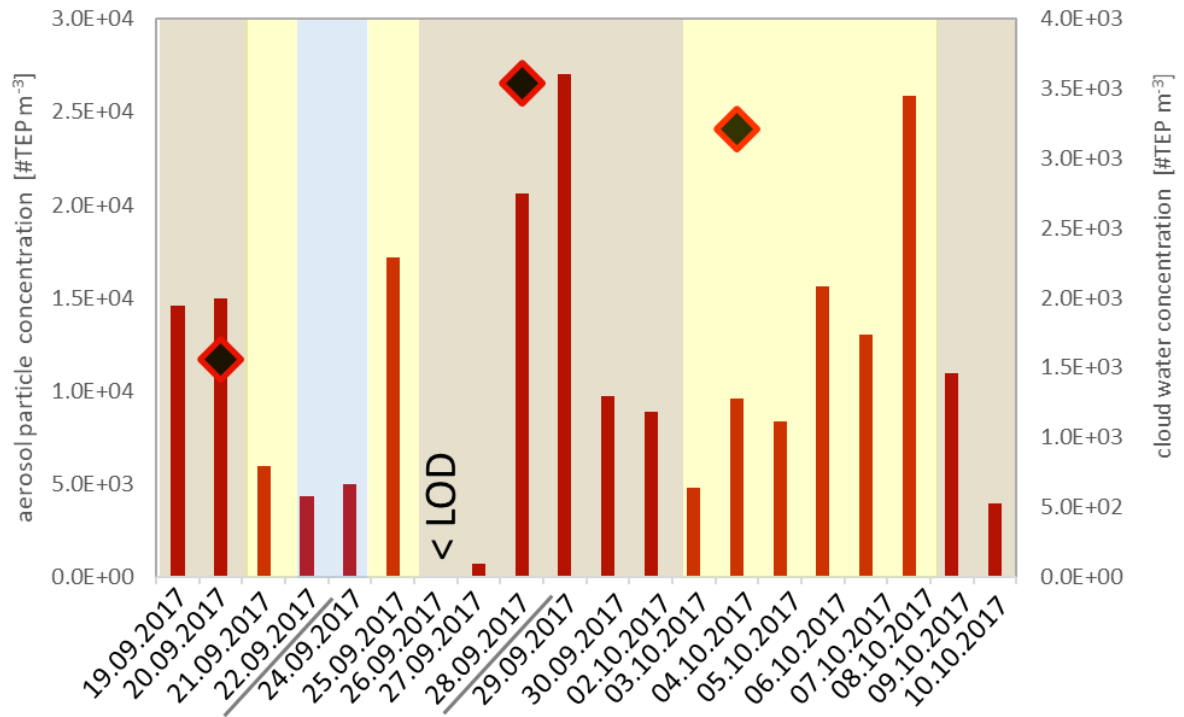


Figure 1



1154
 1155
 1156
 1157
 1158
 1159

Figure 2

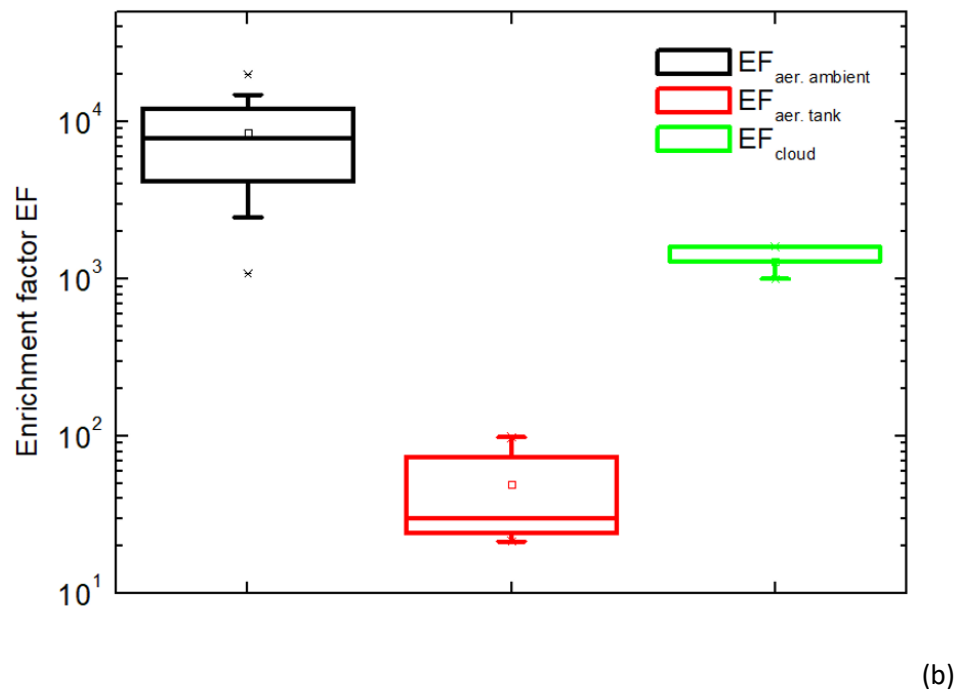
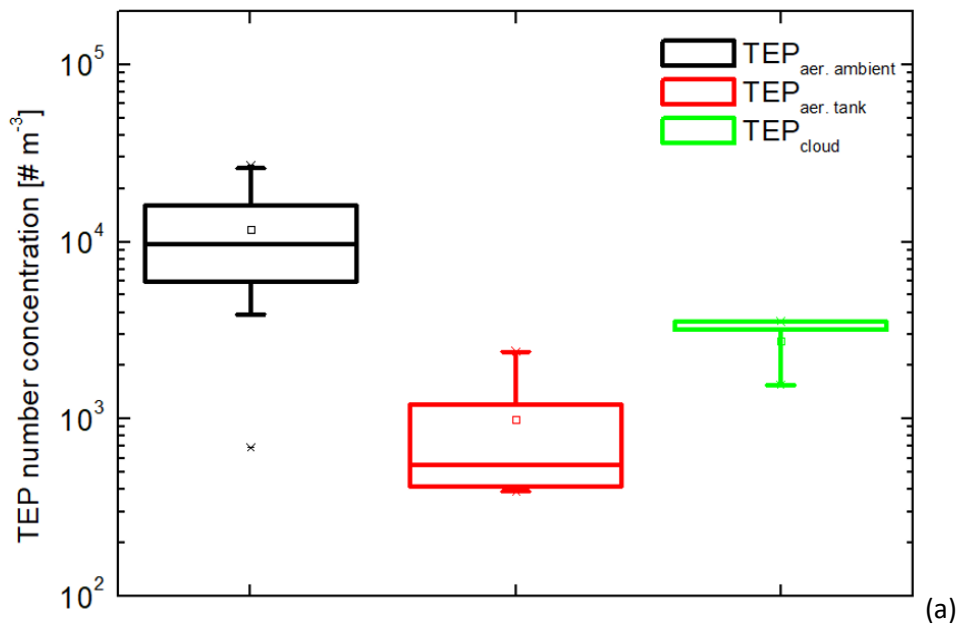
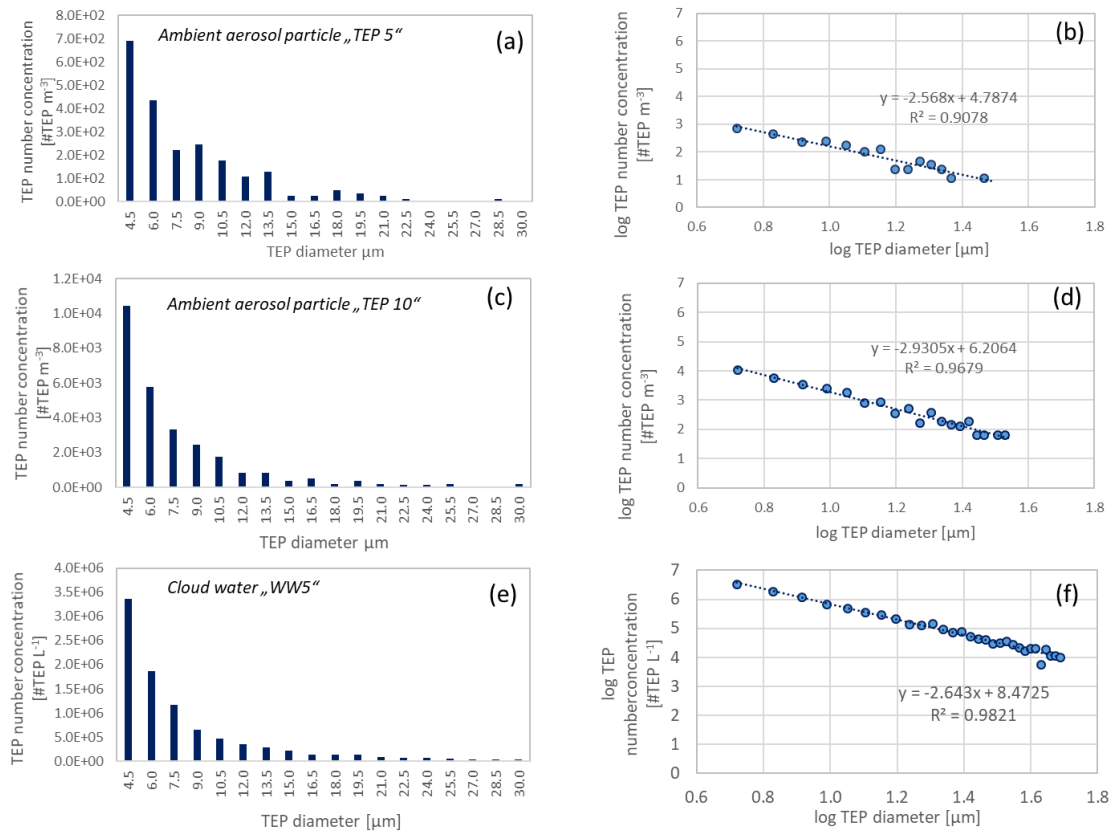


Figure 3

1176

1177



1178

1179

1180

1181

1182

1183

1184

1185

1186

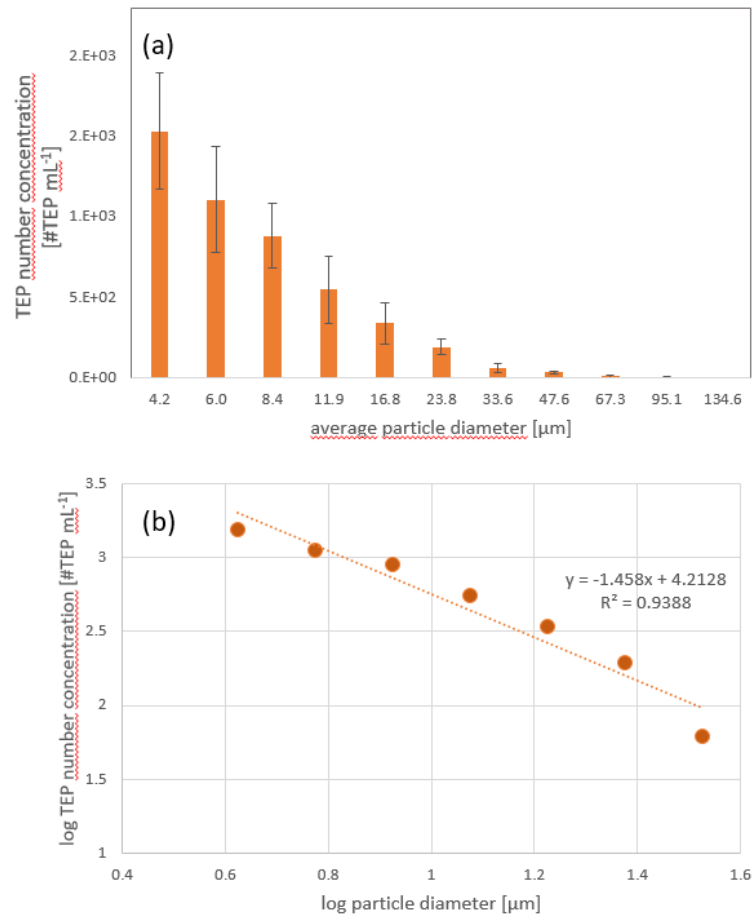
1187

1188

1189

Figure 4

1190



1191

1192

1193

1194

1195

1196

1197

1198

1199

Figure 5

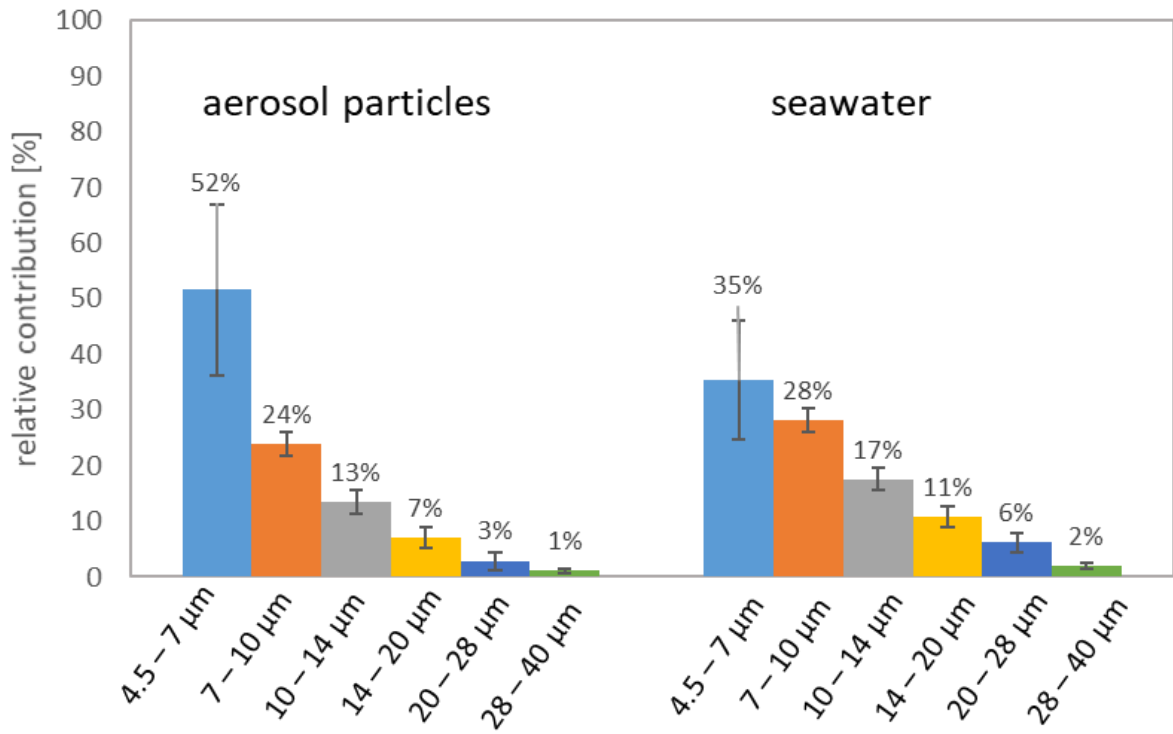
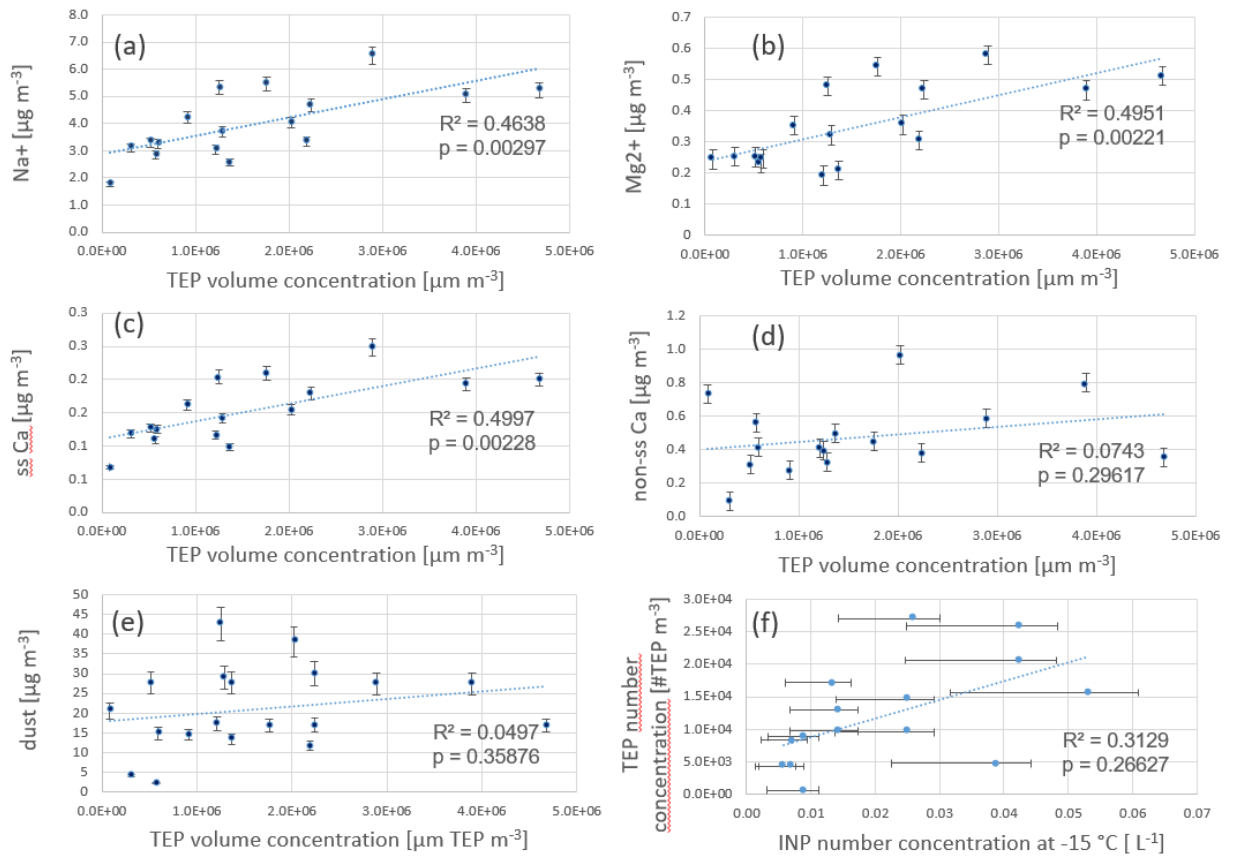


Figure 6

1200
 1201
 1202
 1203
 1204
 1205
 1206
 1207
 1208
 1209
 1210
 1211
 1212
 1213
 1214
 1215



1216

1217

1218

1219

1220

1221

1222

Figure 7